A NEW MODEL OF THE ECLIPSING SYSTEM RZ OPHIUCHI

by

LEWIS BENJAMIN GRAHAM KNEE

B.Sc. (Hon.), Memorial University of Newfoundland, 1983

A THESIS SUBMITTED IN PARTIAL FULFILLMENT OF THE

REQUIREMENTS FOR THE DEGREE OF MASTER OF SCIENCE

in the Department of Physics

We accept this thesis as conforming to the required standard

[redacted]

Dr. Colin D. Scarfe

[redacted]

Dr. Christopher J. Pritchet

[redacted]

Dr. Frank P. Robinson

[redacted]

Dr. Alan H. Batten

[redacted]

Dr. Graham Hill

University of Victoria, August 1985

Supervisor: Dr. Colin D. Scarfe

ABSTRACT

The analysis of new multi-colour photometric observations of the primary eclipse of the binary system RZ Ophiuchi is presented.

The ratio of the radii k of the two stars has been determined using the effective temperature and bolometric correction of each star derived from the photometry, and a photometric solution for the orbital inclination and the radii of each star made using this value. The solution supports the model of RZ Ophiuchi favoured by Baldwin and by Forbes and Scarfe, in which the secondary star does not fill its Roche lobe.

The photometric results were combined with the new radial-velocity solution for this system of Mayor, and the physical parameters of the system determined. A short discussion of the peculiar evolutionary history of the system is presented; it appears that RZ Ophiuchi may be an example of a system in a short-lived phase of Case C mass exchange. A few suggestions for further research are given.

Examiners: [redacted]

Dr. Colin D. Scarfe

[redacted]

Dr. Christopher J. Pritchet

[redacted]

Dr. Frank P. Robinson

[redacted]

Dr. Alan H. Batten

[redacted]

Dr. Graham Hill

TABLE OF CONTENTS

TABLE OF CONTENTS (CONTINUED)

LIST OF TABLES

LIST OF FIGURES

ACKNOWLEDGEMENTS

I owe thanks to many people for their contributions, both direct and indirect, to this thesis. Principally among them, I thank my supervisor, Dr. Colin D. Scarfe, who suggested the project, organized and participated in the observational campaign, and ably and patiently guided my two years of studies and research. Among many other things, he taught me that research consisted of finding out things for oneself, and allowed me to follow my own thoughts and ideas.

I thank also for their cooperation and vital contributions the other collaborators in the observational effort, Dr. Barrow W. Baldwin, Mr. Stephen J. Meatheringham, and Ms. Jocelyne M. V. Gagné.

My visit to Pine Mountain Observatory was a very pleasant and stimulating one. I thank especially Dr. James C. Kemp for granting me unrestricted access to the facilities at Pine Mountain and for his hospitality during my stay there. I thank Mr. Daniel Kraus of Pine Mountain for his friendship, encouragement, and assistance.

I am greatly indebted to Dr. Michel Mayor for making available the results of his new radial-velocity study of RZ Ophiuchi. His was a unique and very valuable contribution to this work.

Thanks also go to Dr. Donald A. VandenBerg, who employed me during my first summer at the University of Victoria and who has often acted in the role of a "second supervisor" through my many discussions with him. His suggestions concerning effective temperature and bolometric correction scales were very useful.

I wish to thank the Natural Sciences and Engineering Research Council for their financial support through an NSERC Postgraduate Scholarship and the University of Victoria for the honour of holding the R. M. Petrie Memorial Fellowship in 1984-85.

The comradeship of the astronomy graduate students at the University of Victoria, Tim Davidge, Carl Grillmair, Dave Holmgren, Polo Infante, Liisa Jylänne, and Rob von Rudloff, is valued deeply by me. Their friendship brightened and enriched my life in Victoria.

CHAPTER 1. INTRODUCTION

1.1 THE ECLIPSING BINARY RZ OPHIUCHI

RZ Ophiuchi is a long period binary system in which Algol-like deep primary eclipses occur when the hot, smaller primary star is occulted by a cooler, larger secondary star. The eclipse is total for approximately 9 days while each of the two partial phases lasts about 30 hours. The orbital period of the system is about 262 days. The secondary eclipse, of the same duration as the primary eclipse, is a transit of the cooler star by the hotter component. Secondary eclipse is expected to be very shallow and has not yet been definitely detected (Baldwin, 1976, Seares, 1908).

The optical spectrum of RZ Ophiuchi displays strong double-lobed hydrogen Balmer emission lines which are present throughout the orbital period of the system, and which show an "eclipse effect" which is interpreted as the partial eclipse by the secondary component of an extensive flattened disk or ring of gas surrounding the primary star (Hiltner, 1946). The disk is bright enough so that its eclipse can be detected photometrically outside stellar eclipse (van Paradijs et al., 1982). van Paradijs et al. found the disk eclipse to have a duration of 42 days, which has been confirmed by photopolarimetric observations of the June 1984 primary eclipse (Kemp, 1984). Small out-of-eclipse brightness variations of RZ Ophiuchi may be due to the disk (Olson, 1984, Olson and Hickey, 1983).

Plavec (1980) has speculated that RZ Ophiuchi may be a member of his class of "W Serpentis" long period systems in which a high mass transfer rate results in an accretion disk surrounding one star.

1.2 THE ROCHE MODEL OF BINARY SYSTEMS

One of the most useful systems for the classification of binaries, especially in close (interacting) binaries, is based on the Roche model. In most theoretical investigations of the interaction of two stars through mass transfer and its evolutionary effects this model is used. Although it is a somewhat idealized model, it has found wide applicability.

Assume both stars in a system are Newtonian point masses in a circular orbit and that their rotation is synchronous with the orbit. The gravitational equipotentials surrounding each star will be nearly spherical close to the centre of each component, as seen in a reference system rotating with the components around the centre of mass of the system. As the size of the equipotentials increases, they begin to distort to form dumbbell-shaped lobes with the long axes pointed along the line between each star. For a certain value of the gravitational potential, the two distorted lobes will touch each other at a point between the components called the inner Lagrangian point L_1. This equipotential surface is the critical Roche surface or the critical Roche lobes. Equipotential surfaces outside this critical surface suffer further distortion. At a greater distance another equipotential surface

will intersect itself at the outer Lagrangian point L_2 directly behind the less massive star. This surface is the outer critical surface. See figure 1 for a sketch of the Roche geometry.

The components of a binary can be classified as either filling (a "contact" component) or not filling (a "detached" component) its critical Roche lobe. A star whose surface remains inside its critical surface will not transfer any significant mass to its companion (unless it has a strong stellar wind or a very extended atmosphere), but if it fills or spills over this surface significant mass transfer to the other star can occur through the inner Lagrangian point.

A system in which one component fills its critical surface is "semi-detached", and a system in which both fill their critical surfaces is a "contact" system. If both stars lie below their critical surfaces, the system is "detached".

A contact system can overflow the inner critical surface, but if it fills the outer critical surface mass can be lost from the system through the outer Lagrangian point.

1.3 BALDWIN'S MODEL OF RZ OPHIUCHI

The first major observational study of RZ Ophiuchi since the early part of the 20th century was presented by Baldwin (1976, 1978) from severely limited photometric observations of two primary eclipses, spectroscopic radial-velocity measurements throughout the orbital cycle, and spectroscopy of the hydrogen emission lines.

FIGURE 1: THE ROCHE GEOMETRY OF A BINARY SYSTEM

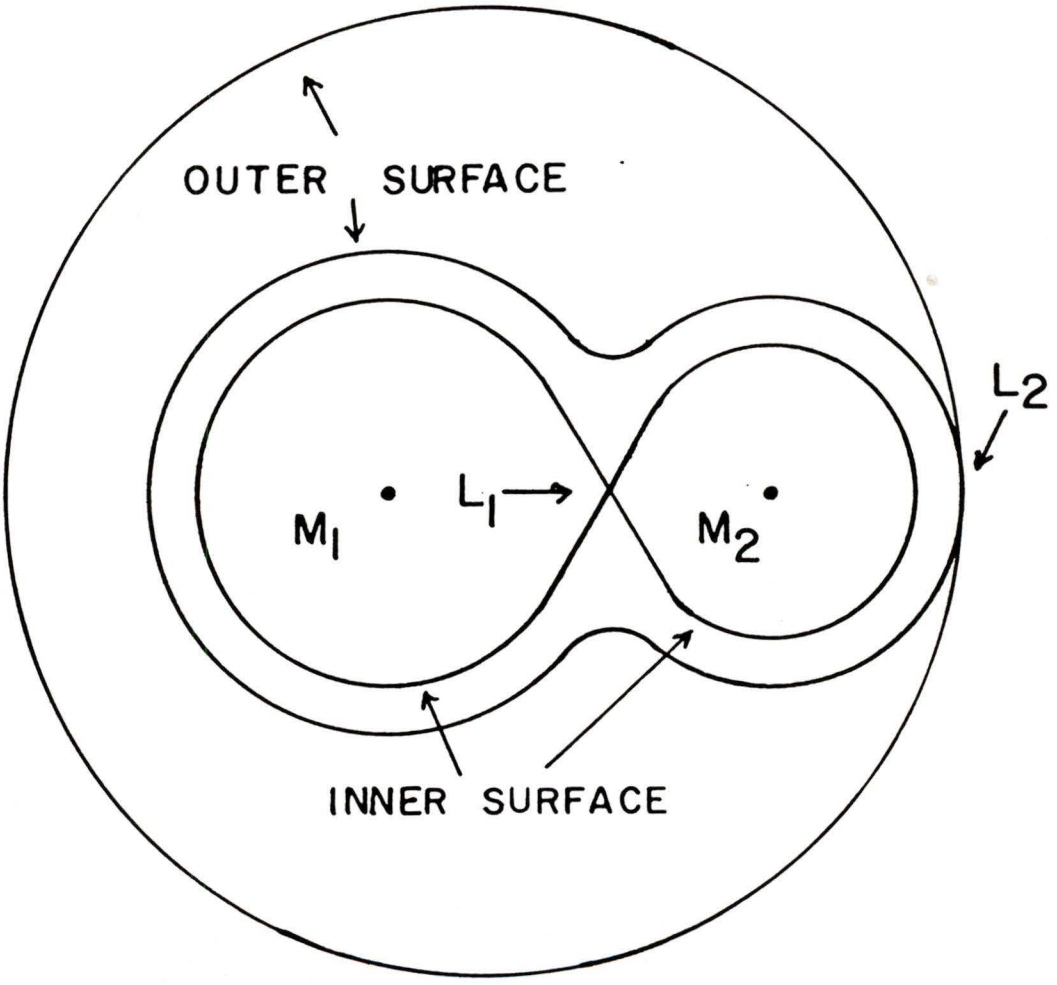

He obtained preliminary photometric and spectroscopic elements and a somewhat poorly determined mass ratio, and presented a model of the circumstellar disk. His study of all available eclipse timings showed that the orbital period had remained constant at P = 261.9277 days ± 0.0029 days since the star's variability was first discovered in 1905, and he calculated an ephemeris.

Baldwin estimated the depth of the eclipse in the B and V bands and the phases of the eclipse contacts. Insufficient data to permit a photometric solution for the geometric parameters forced Baldwin to assume an inclination of 90°. The ratio of the stellar radii could then be determined by comparison of the durations of the partial and total phases of the eclipse.

The masses and radii he determined for the two stellar components indicated that the less massive, and therefore slowly evolving cooler star was in a more advanced state of evolution than the more massive, quickly evolving primary. This situation is the well-known "Algol paradox", and it can be resolved by invoking mass transfer from the initially more massive star to the less massive star when the former overflows its critical Roche lobe. Rapid mass transfer can then invert the mass ratio, and by the time the mass-losing star has shrunk back to its critical lobe, the previously less massive star is now the more massive, hotter component while the mass-losing star is cooler and fills its critical surface (Crawford, 1955, Morton, 1960).

Thus, the presence of a circumstellar disk around the hotter star, and the cooler, less massive secondary, would suggest that mass transfer

from the secondary to the primary is responsible for the present state of the system. The secondary star would then be expected to fill its critical Roche lobe, but in Baldwin's model the secondary's radius is only half that. This left the question of the evolutionary history of RZ Ophiuchi and the origin of the large disk somewhat mysterious.

1.4 SMAK'S MODEL OF RZ OPHIUCHI

Smak (1981) reanalyzed the data of Baldwin and criticized his model of the two stellar components and the disk. Included in Smak's discussion of the problems in the earlier work was a criticism of the assumption that the inclination of the orbital plane was 90°, and he noted that it led to the too-small radius of the secondary and hence to the evolutionary problem.

Instead of assuming a value for the inclination, Smak chose an alternative tactic of assuming that the secondary did fill its critical Roche surface, and deduced a new set of geometric parameters which included a significantly smaller inclination of 75.5°. This rather low inclination implied that the total eclipse is very nearly grazing.

Smak noted that the radius found for the smaller star was very sensitive to the choice of the phases of contact, and used different but plausible values (given the poor light curves) to arrive at his semi-detached model of RZ Ophiuchi.

Thus Smak's model could attribute the origin of a large disk around the hotter star and the evolutionary state of the two components to mass

transfer from the lobe-filling secondary to the primary.

1.5 THE WORK OF FORBES AND SCARFE

In an effort to resolve the dilemma of the model of RZ Ophiuchi, Forbes and Scarfe (1984) conducted a new photometric study and combined their observations with those of Baldwin and those of Barlow (unpublished). They were forced to rely on the spectroscopic orbits and mass ratio of Baldwin since no new observations were available.

They pointed out that Smak's assumption regarding the radius of the secondary star was also somewhat arbitrary, and attempted to perform a photometric solution to determine the inclination and radii instead of assuming one or the other. However, the problem of adequately covering the long partial phases of the eclipse from one location, even though data from several eclipses were available, hampered their attempts to compare Baldwin's and Smak's models with the eclipse light curves. They were able to rule out Smak's phases of eclipse contacts, but the combination of fairly high inclination and small ratio of the radii of the components made the light curves predicted by each model nearly identical.

Unable to distinguish between the two models through the eclipse photometry, Forbes and Scarfe compared the masses, radii, and surface gravities of the two stars resulting from each. They found that the spectral types, relative visual luminosity, and the difference in the bolometric corrections of the two stars all seemed to be consistent in

Baldwin's model but not so in Smak's. Forbes and Scarfe hence favoured Baldwin's analysis, though it was clear that a completely satisfactory solution remained out of reach due to the still severely limited observational data.

1.6 THE OBJECTIVES OF THIS STUDY

To make any further substantial progress in understanding this enigmatic system, a number of observational objectives need to be reached, as pointed out by Forbes and Scarfe. They are:

(1) Improved photometry of the eclipse light curves by improved coverage of the partial phases. The only way of achieving this during a single eclipse is to have a number of observers distributed widely over longitude.

(2) Accurate eclipse depths in U, B, and V to determine the relative luminosities and colours of the two stars more accurately.

(3) Determination of the R and I magnitudes of each star in order that their bolometric corrections and effective temperatures can be better determined. This would allow the ratio of the radii to be determined independently of the photometry, and thus help distinguish between the two models.

(4) An improved determination of the mass ratio. Since the size of the critical Roche lobes are dependent upon them, a better mass ratio is vitally important. This would require new radial velocity

observations over the full cycle, leading to more reliable spectroscopic orbits for the components than those obtained by Baldwin.

With these points in mind, a campaign was launched to observe the June 1984 primary eclipse of RZ Ophiuchi with the aim of achieving as many as possible of the first three above goals, and in so doing shed light on the present state and past history of this system.

CHAPTER 2. THE OBSERVATIONAL EFFORT

2.1 PHOTOELECTRIC PHOTOMETRY

It is appropriate to present a short description of astronomical photoelectric photometry before going on to an account of the observational effort. Complete discussions of the technique are given by Hall and Genet (1982), Henden and Kaitchuck (1982), and Young (1974). Only an outline of the physics and design of photoelectric photometers is presented here. An account of the observing and reduction techniques follow in subsequent sections.

Photoelectric photometry is one of the fundamental methods of measuring the apparent brightness and colour of astronomical objects. The first experiments with selenium photocells took place at the end of the 19th century, but modern photoelectric photometry was born at the end of the Second World War with the introduction of the photomultiplier tube.

The photomultiplier operates on the principle of photoemission in a vacuum (the external photoelectric effect). A photocathode is coated with a photosensitive surface usually composed of a semiconducting alloy. When a sufficiently energetic photon is absorbed by the surface, an electron can be emitted. Since the probability per absorbed photon of electron emission is constant, the electron current from the photocathode is directly proportional to the light intensity. Thus, measurement of the current results in a measurement of the brightness of

the observed light source (a star, for example).

The extremely small current produced (approximately 10^{-15} ampere) must be greatly amplified if it is to be measured. The electronic amplification of such a tiny photocathode current would result in an unacceptably noisy signal. The use of electron multipliers provides a way to amplify the current without resulting in significant degradation of the signal (Lallemand, 1962).

Electron multiplication in the tube is accomplished by directing the electron current onto a series of targets ("dynodes") using electric and/or magnetic fields. The dynodes are coated with substances (often alloys or oxides of alkali metals) that emit large numbers of electrons when bombarded with energetic electrons. The current is greatly amplified by directing it from one dynode to another in a "cascading" effect. In typical photomultipliers containing 10 to 20 dynodes, the original current can be increased by a factor on the order of a million. The output current from the photomultiplier (now about 10^{-8} or 10^{-9} ampere) can be further amplified electronically and measured.

The components of a basic single-channel photometer are shown in figure 2 (see Johnson, 1962). Most photometers are designed to be used at the Cassegrain focus of the telescope due to their relative ease of construction, mounting, and use. One or two eyepieces will be used for object-finding and/or guiding. The mirrors that direct the light beam into the eyepieces are moved out of position so that the beam will enter the photomultiplier tube during the observation. A focal-plane diaphragm is used to isolate the image of the object to be observed. Following the

FIGURE 2: BASIC SINGLE-CHANNEL PHOTOMETER

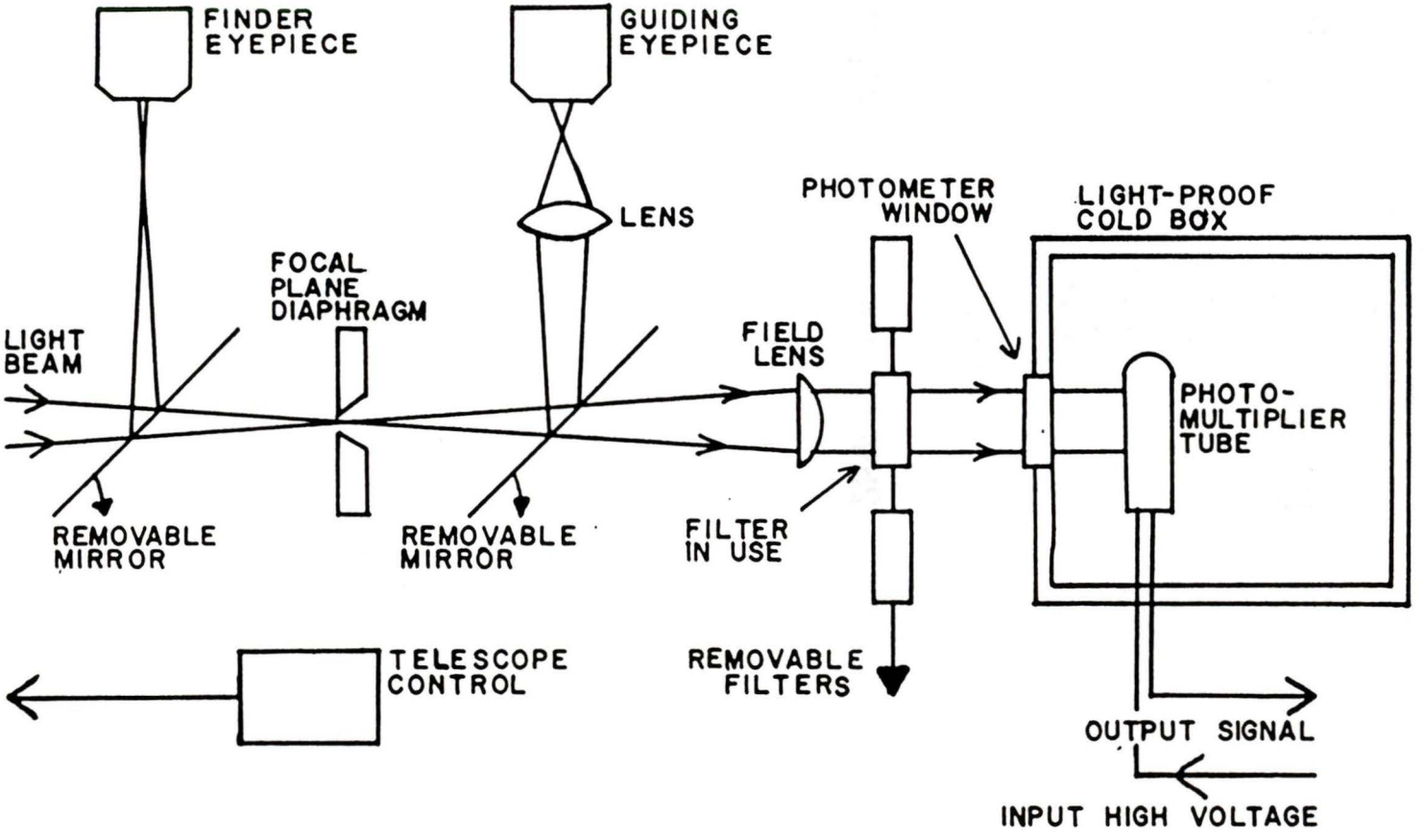

field lens is a filter used to block all but a chosen range of wavelengths from entering the photomultiplier. This permits brightness measurements to be made in different parts of the spectrum, and photometric colours determined. The photomultiplier tube is housed in a light-tight box which is usually cooled by dry ice or liquid nitrogen in order to reduce the "dark current" (noise produced mostly by thermionic emission in the tube or by gaseous ions). The current from the photomultiplier can be amplified and recorded using two different methods, the direct-current (DC) or the pulse-counting technique.

The DC method is relatively straightforward and was the first to be used in astronomical photometry. The output from the photomultiplier is amplified and smoothed by a DC operational amplifier and the current is recorded on a chart. This technique has the disadvantage that the signal-to-noise ratio which can be achieved is limited, so observations of very faint astronomical sources are very difficult. In addition, the analogue nature of the output makes data reductions laborious. These problems can be overcome somewhat by using analogue-to-digital electronics to convert the output signal to digital form. This permits integration of the signal and hence greater signal-to-noise ratios. In conventional DC photometry, the amplifier gains can be set by the observer to obtain comparable chart pen deflections for stars of different brightnesses. These gain settings are usually expressed in magnitudes. Since amplifier drift can occur, it is necessary to calibrate the gain settings at the telescope against a standard.

Pulse-counting electronics amplify and count individual electron

pulses from the photomultiplier (integrating the signal). Each pulse signals the detection of one photon by the photocathode, and thus this type of photometer is a photon-counting system. Pulse-counting allows high signal-to-noise ratios to be attained, which is especially important when faint sources are observed or if greater accuracy is desired. Since pulses are counted rather than current measured, amplifier drift is not a problem. One problem encountered is that the detection of two or more pulses spaced very closely in time is difficult, due to the "dead-time" of the counting electronics. The dead-time is the period of time that it takes for the electronics to "recover" from one pulse and return to a state in which it is able to detect another. The correction for dead-time must be determined for the individual systems used, especially if relatively bright stars are to be observed.

More sophisticated photometer systems than the simple single-channel system described here are in operation around the world. Dual- or multi-channel photometers are capable of simultaneous observations of different fields and/or in different colours. For example, simultaneous star and sky measurements increase accuracy by accounting for short-term sky variations. The single-channel "chopping" photometer, which switches rapidly between two diaphragm fields, can perform the same function. Light detector arrays (such as charge-coupled devices) are increasingly being used to perform simultaneous multi-object photometry. These devices use two-dimensional arrays of solid-state detectors rather than a photomultiplier tube.

2.2 DIFFERENTIAL PHOTOMETRY OF VARIABLE STARS

To obtain accurate photometry and place the results on a standard system of magnitudes and colours, a number of tasks must be completed at the telescope:

(1) A measurement of the brightness of a star will include the contribution of the sky background included in the photometer diaphragm. To obtain measurements of the star alone, the sky brightness should be measured frequently (bracketing the stellar observations). Then during the reductions, the sky background can be interpolated and subtracted.

(2) Atmospheric extinction is the absorption of light by our atmosphere. The amount of extinction depends on how much atmosphere the telescope looks through to observe a star, hence it varies with the altitude of the star. Extinction is wavelength-dependent (hence different in each band) and depending on the behaviour of airborne dust and aerosols, temperature, or air pressure, can vary slowly as a function of time and/or position in the sky. The amount of extinction present must be determined by observing a star in different colours over a wide range of zenith distance, and the photometry then corrected for its dimming effect. The extinction in each band has a second-order colour effect which can be determined by observing extinction stars with different intrinsic colours.

(3) The spectral response of the filters used, as well as the spectral

response and sensitivity of the photometer and the telescope optics will all define a unique "natural system" of magnitudes and colours. To compare measurements taken with other telescopes, transformation of results to an agreed-upon "standard system" must be made. This requires the observation of several stars whose standard magnitudes have already been determined.

(4) In pulse-counting, correction for dead-time must be made, especially for bright stars. This correction is usually determined in advance of the observing session (see Henden and Kaitchuck).

(5) In DC photometry (unless in A-to-D mode) the gain settings must be recorded for later use in the reductions. As noted previously, the gain scales must be calibrated against a standard source (such as a radium source).

(6) The time of the observations must be recorded, usually in UT.

(7) Filters for use in the ultraviolet typically will also transmit a small amount of red light which contaminates the ultraviolet observations. If steps have not already been made to suppress this "red leak", it will need to be measured during the observations and subtracted during the reductions.

The method of differential photometry is often favoured by astronomers because it is a relatively easy way to obtain results of very high accuracy (on the order of a few thousandths of a magnitude). In this method observations are made of the variable star of interest and also a nearby (less than 0.5° distant if possible) non-varying star

called the "comparison star". The photometric measurements can then be expressed as a magnitude difference between these two stars. This allows greater accuracy, particularly if the comparison star is well-chosen. The principal advantages of using a good comparison star are:

(1) If the comparison star is close to the variable the effects of atmospheric extinction on the brightness measurements of the variable, including temporal and spatial variations, will be largely done away with. A comparison star with roughly the same colours as the variable will ensure that the second-order colour dependence of extinction is also small, and this effect is often neglected.

(2) Since it is necessary to observe the comparison star throughout the night, its photometry can also be used to determine the atmospheric extinction. Determination of the extinction coefficients is necessary in the reduction of the standard star observations.

(3) If the comparison star is about the same brightness as the variable, then the same gain settings can be used (in DC photometry) for the variable and the comparison star observations, hence reducing any potential problems in their calibration (such as gain variations during the night). In pulse-counting photometry the effects of dead-time can be greatly reduced if the variable and comparison stars are about the same brightness.

It is also desirable to measure occasionally throughout the night

another nearby star, the "check star". Comparison between the check and comparison star photometry is a good way to ensure that the comparison star is not variable itself and is also a useful way to monitor the photometric quality of the night. Sometime during the night (often halfway through the observing session) observations of the standard stars are performed, so that the transformation of the variable star photometry in the natural system to a standard system can be made.

The basic procedure outlined above was followed by all of the observers involved in the photometric campaign.

2.3 REDUCTION OF THE PHOTOMETRY

The reductions followed the procedure described by Hardie (1962). Steps 1 to 5 below describe the initial reductions of the variable, comparison, and check star data, and the determination of extinction.

(1) If the photometry is in chart recorder form, the tracings are measured, noting the gain scales used in each case. The gain scales are calibrated in magnitudes. If pulse-counting or A-to-D DC photometry is used, the observations are reduced to equal integration times (such as counts per second). If pulse-counting is used, the dead-time correction is applied to all of the observations by solution of the transcendental equation:

$$n = N e^{-Nt} \qquad (1)$$

where n is the observed count rate, N is the corrected rate, and t

is the dead-time e-folding constant for the particular system used.

(2) For each stellar measurement the bracketing sky backgrounds are interpolated and subtracted. This removes the sky light from the photometry. The red-leak is subtracted from the ultraviolet observations.

(3) For each variable star measurement, the bracketing comparison star measurements are interpolated. Then the differential magnitude Δm of the variable star is:

$$\Delta m = m_v - m_c = -2.5 \log (N_v/N_c) \qquad (2)$$

where m_v and m_c are the natural magnitude of the variable and comparison star respectively, and N_v and N_c are the corresponding measured count rates (in pulse-counting or A-to-D DC systems). If conventional DC photometry is being reduced, this expression is slightly altered:

$$\Delta m = -2.5 \log (N_v/N_c) + G_v - G_c \qquad (3)$$

where now N_v and N_c are the measured current levels and G_v and G_c are the calibrated gain settings (in magnitudes) of each measurement.

(4) Equation 2 or 3 is used in a similar way to determine the differential magnitudes of the check star. Then the constancy of the comparison star and the quality of the night can be assessed.

(5) The extinction coefficients need to be determined in order to reduce the standard star photometry. The magnitude of a star suffering extinction is given by (to first order only):

$$m = m_0 + KX \qquad (4)$$

where m_0 is the magnitude the star would have if there were no extinction, K is the extinction coefficient for the spectral region in which the star was measured, and X is the "air-mass" of the observation. K determines the amount of extinction (in magnitudes per air-mass) present on a given night and its value must be determined. The air-mass is the amount of atmosphere in the line of sight to the star expressed in terms of the air-mass at the zenith, and is given to an excellent approximation (see Young) by:

$$\sec z = (\sin \phi \sin \delta + \cos \phi \cos \delta \cos H)^{-1} \quad (5)$$

$$X = \sec z \, (1 - 0.0012 \tan^2 z) \quad (6)$$

where ϕ is the observer's latitude, δ is the declination of the star, and H is the hour angle of the star. To determine K in each filter, the magnitude of the comparison star is plotted versus X. The slope obtained will give K and the intercept will be m_0 for the comparison star. Figure 3 presents an example of the determination of extinction in the standard B band for observations of the comparison star to RZ Ophiuchi. These observations were obtained on the night of June 24/25 1984 by Dr. C. D. Scarfe at Lick Observatory.

For the variable and comparison star X_v and X_c are nearly equal, so that (providing we can neglect second-order extinction):

$$m_v - m_c = (m_{vo} + KX) - (m_{co} + KX) \quad (7)$$

or:

$$m_v - m_c = m_{vo} - m_{co} = \Delta m \quad (8)$$

FIGURE 3: EXAMPLE OF DETERMINATION OF EXTINCTION COEFFICIENTS

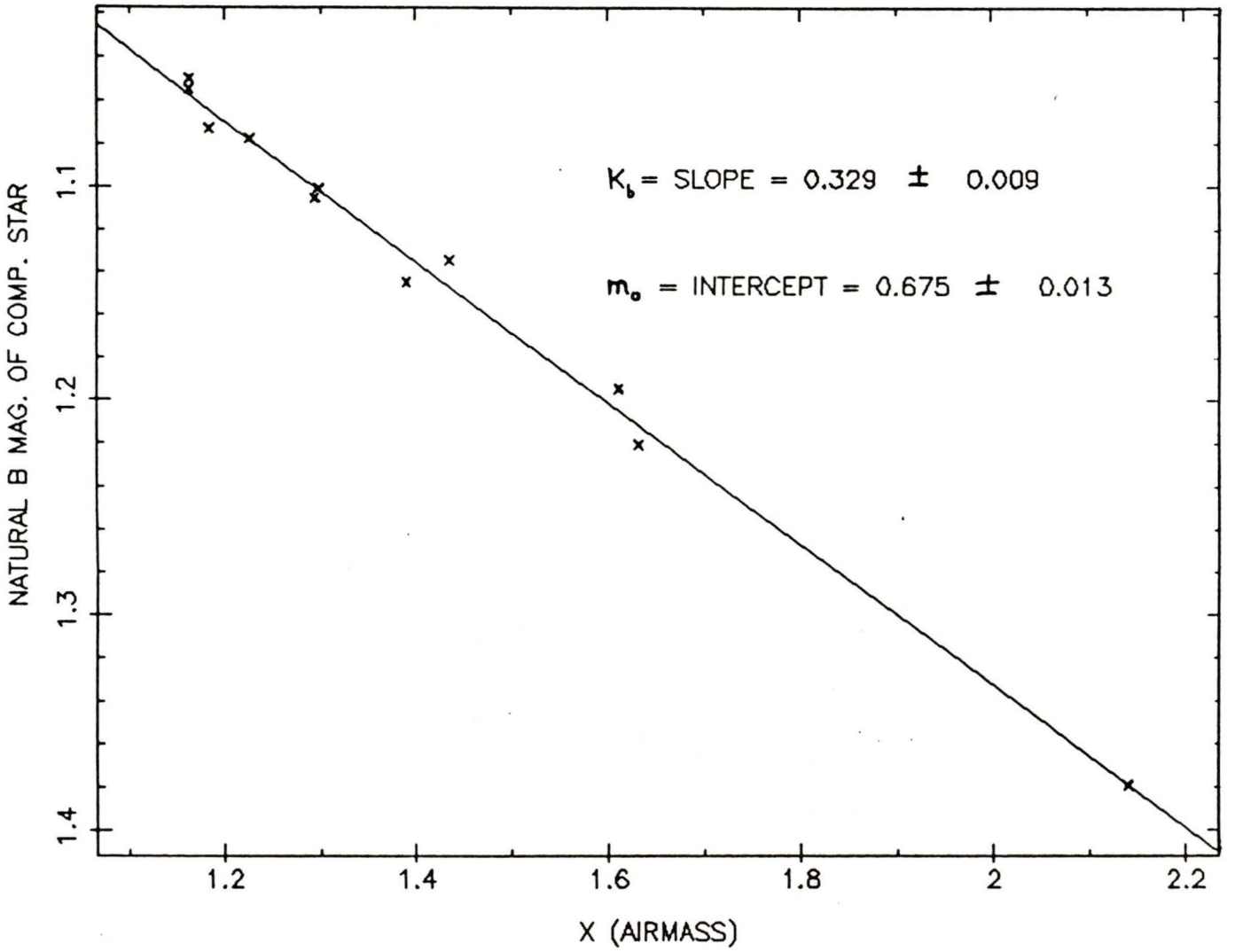

This confirms that extinction can be ignored when calculating the differential magnitudes of the variable and check star with respect to the nearby comparison star.

Steps 6 to 8 describe the reduction of the standard star observations to the natural system, corrected for extinction.

(6) For each standard star observation, steps 1 and 2 above are performed.

(7) Magnitudes in the natural system (uncorrected for extinction) are then calculated by (for digital data):

$$m = -2.5 \log N \tag{9}$$

or (for chart recorder data):

$$m = -2.5 \log N + G \tag{10}$$

where the symbols are defined in a like manner as in equations 2 and 3. Note that these are not differential magnitudes.

(8) The observations are corrected for extinction using the extinction coefficients determined in step 5:

$$m_0 = m - KX \tag{11}$$

where X is the air-mass of the observation, as before.

The determination of the transformation between the natural and the standard system is most easily described by using the notation of the system used in this study, namely the UBVRI system defined by Landolt (1973, 1983).

(9) The relationships between the colours and magnitudes in the natural system and those in the standard UBVRI system are:

$$V = \varepsilon\ (B - V) + v_0 + \zeta_v \tag{12}$$

$$U - B = \phi\ (u_0 - b_0) + \zeta_{ub} \tag{13}$$

$$B - V = \mu\ (b_0 - v_0) + \zeta_{bv} \tag{14}$$

$$V - R = \xi\ (v_0 - r_0) + \zeta_{vr} \tag{15}$$

$$R - I = \eta\ (r_0 - i_0) + \zeta_{ri} \tag{16}$$

where the Greek symbols are the "transformation coefficients" and the ζ's are the "zero points". In the case of the standard stars, the values of the quantities on the left-hand side of these transformation equations are known, and the corresponding values (the lower case symbols) have been measured through the standard star photometry. Determining the transformation coefficients and the zero points is then a matter of a linear regression analysis of each of equations 12 to 16. Figure 4 illustrates this procedure using the standard star observations of June 24/25 made at Lick. The known B-V colours of the standards are plotted against the observed b_0-v_0 colours. The slope of the linear relation between the two quantities gives the transformation coefficient μ and the intercept gives the zero point ζ_{bv}.

(10) It can easily be shown that differential magnitudes in the standard system are then given by:

$$\Delta V = (1 - \varepsilon\mu)\ \Delta v_0 + \varepsilon\mu\Delta b_0 \tag{17}$$

$$\Delta B = \Delta V + \mu\ (\Delta b_0 - \Delta v_0) \tag{18}$$

$$\Delta U = \Delta B + \phi\ (\Delta u_0 - \Delta b_0) \tag{19}$$

FIGURE 4: EXAMPLE OF DETERMINATION OF TRANSFORMATION COEFFICIENTS

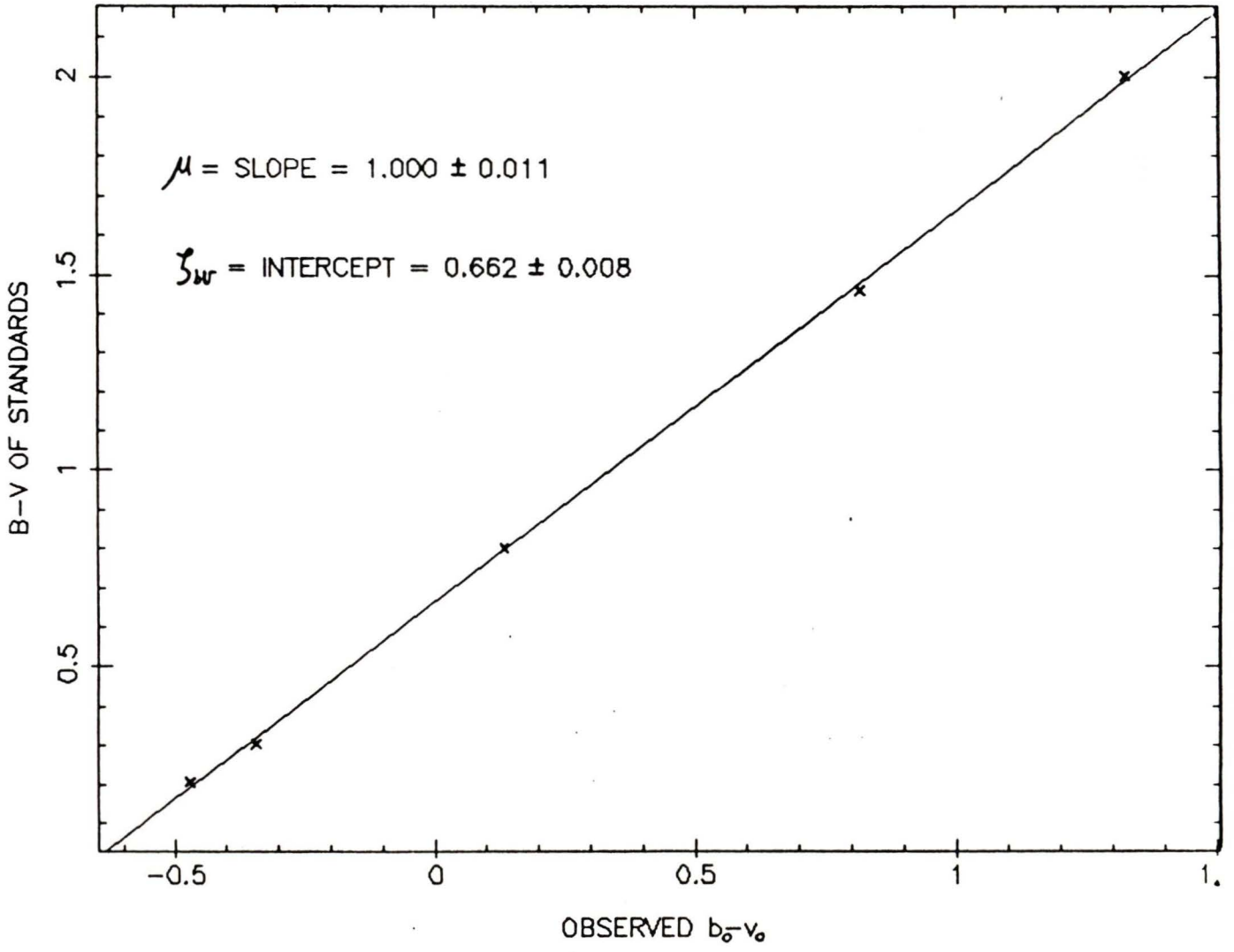

$$\Delta R = \Delta V - \zeta\ (\Delta v_0 - \Delta r_0) \qquad (20)$$

$$\Delta I = \Delta R - \eta\ (\Delta r_0 - \Delta i_0) \qquad (21)$$

Using equations 17 through 21, the differential magnitudes of the variable star with respect to the comparison star are calculated. The comparison and check stars can be placed on the standard system using equations 12 through 16. Then it is a simple matter to place all of the variable star observations in the UBVRI system as well. This completes the reductions.

It should be noted that the transformation coefficients depend on the characteristics of the filters used as well as the spectral response of the photometer, thus they are expected to be fairly constant from night to night. However, the zero points depend on the behaviour of the telescope optics and the absolute sensitivity of the photometer, both of which may vary slightly from night to night. It is thus important to determine at least the zero points every night.

2.4 THE PHOTOMETRIC CAMPAIGN

The time of mid-eclipse and the phases of the contacts of the 1981 summer eclipse determined by Forbes and Scarfe were used to make approximate predictions of the time of the contacts for the eclipse of June 1984. Baldwin's orbital period was assumed. Forbes and Scarfe estimated first and fourth contacts to occur at about -6.1 days and +6.1 days respectively, and second and third contacts to occur at

-4.9 days and +4.9 days respectively (mid-totality is defined as zero phase, and the time of the contacts measured with respect to it). The predictions based on this ephemeris are found in table 1. No uncertainties in the predictions are quoted, but inspection of the light curves of Forbes and Scarfe suggest they may be as high as ± 12 hours.

The comparison (BD+06° 3917) and check (BD+06° 3918) stars chosen were those used by both Baldwin and Forbes and Scarfe. They are both less than 0.5° from RZ Ophiuchi and somewhat brighter. The colours of the comparison star are similar to those of RZ Ophiuchi out-of-eclipse, while the check star colours are redder, as is RZ Ophiuchi during totality. The positions of these three stars, plus the V magnitudes determined by Forbes and Scarfe, are found in table 2.

The standard stars to be observed were chosen in the nearby Selected Areas 109, 110, and 111 from the list published by Landolt (1983). The colours of RZ Ophiuchi change substantially during eclipse; hence care was taken to ensure that the selected standard stars also covered a large range of colours, in order to provide a reliable set of transformations.

As noted earlier, good coverage of the partial phases of the eclipse required the collaboration of observers worldwide, hence a network of cooperating observers was established, largely through the efforts of Dr. Scarfe. The predictions in table 1, the finding charts for RZ Ophiuchi and the comparison and check stars, as well as a list of suggested standard stars were distributed to the collaborators. The observers who took part in the photometric campaign were the author, Dr.

TABLE 1: PREDICTIONS OF ECLIPSE EVENTS IN JUNE 1984

EVENT	TIME (JULIAN DATE)
FIRST CONTACT	2 445 865.1
SECOND CONTACT	2 445 866.3
MID-TOTALITY	2 445 871.2
THIRD CONTACT	2 445 876.1
FOURTH CONTACT	2 445 877.3

TABLE 2: STELLAR POSITIONS AND APPROXIMATE V MAGNITUDES

STAR	α (2000)	δ (2000)	V (MAGNITUDES)
RZ OPHIUCHI	18h 45m 47s	+07° 13' 11"	9.87 - 10.57
BD+06° 3917	18h 44m 54s	+07° 01' 17"	9.31
BD+06° 3918	18h 44m 56s	+07° 08' 08"	9.13

Barrow W. Baldwin, Dr. Colin D. Scarfe, Mr. Stephen J. Meatheringham, and Ms. Jocelyne M. V. Gagné. The dates of observation and the photometric bands used by each observer are found in table 3, and the standard stars observed are listed in table 4 (The transformation coefficients for the observations of Gagné were determined by Mr. Russell M. Robb and the author). Short notes on the observations made by each collaborator follow.

(1) The author spent 15 days as a visiting guest observer at Pine Mountain Observatory, which is owned and operated by the University of Oregon. A DC photometer operating in an A-to-D mode mounted on a 0.8 metre Sigma 7 Cassegrain reflector was used to make observations in the B and V bands. The S11-type photomultiplier was cooled thermoelectrically, and most of its functions were controlled by a Monroe 1880 microcomputer. Data were recorded on a thermal printer. The telescope movement was under complete computer control and it was programmed to perform a continuous series of observations of the variable, comparison, and check stars, and the sky. Fine guiding of the telescope was done with the use of an RCA television system. The standard stars were observed with the telescope operating in a "manual" mode. An extensive series of observations was made covering parts of the out-of-eclipse, ingress, egress, and total phases. Data reduction was performed on a VAX 11/750 computer at the Department of Physics of the University of Victoria.

TABLE 3: OBSERVERS, FILTERS USED, AND DATES OF OBSERVATION

OBSERVER	FILTERS USED	DATES OF OBSERVATION (JD - 2 440 000)
L. K.	B, V	5863, 5865, 5866, 5869, 5870, 5872, 5875 - 5877
L. K.	B, V, R, I	5908, 5920, 5933
B. B.	U, B, V	5863, 5864, 5866 - 5868, 5874, 5875, 5877, 5878, 5880
C. S.	U, B, V	5865, 5876
S. M.	U, B, V	5865, 5866, 5874, 5876, 5877
J. G.	B, V, R, I	5865, 5868

TABLE 4: STANDARD STARS OBSERVED

STAR	OBSERVER (* = STAR OBSERVED)			
	L. K.	B. B.	C. S.	S. M.
HD 170493				*
HD 173637				*
HD 175544				*
SA 109 231	*	*	*	
SA 109 537	*	*		
SA 109 747	*	*	*	
SA 109 1082	*	*	*	
SA 110 340	*	*		*
SA 110 353	*	*	*	*
SA 110 471	*	*		*
SA 111 717	*	*		
SA 111 773	*	*	*	
SA 111 775	*	*		
SA 111 1496	*	*		
SA 111 1969	*	*		
SA 111 2009	*	*		
SA 111 2522	*	*		
SA 111 2864	*	*		

(2) The author also made some out-of-eclipse observations in the B, V, R, and I bands using the facilities of Climenhaga Observatory described in (6) below. These observations were intended primarily to obtain information on the R and I magnitudes of RZ Ophiuchi outside eclipse. These observations were also reduced at the University of Victoria.

(3) Dr. Baldwin performed observations using the 1.0 metre telescope at Catania Astrophysical Observatory at Serra La Nave, Sicily. He obtained a large number of UBV observations during eclipse and out-of-eclipse phases. Dr. Baldwin reduced his observations on an IBM-compatible PC microcomputer.

(4) Dr. Scarfe made UBV observations during ingress and egress using the DC photometer (cooled by dry ice) on the 0.6 metre reflector of Lick Observatory. The tracings were measured by the author and the subsequent reductions were done on the VAX computer.

(5) Mr. Meatheringham at Siding Spring Observatory in Australia obtained UBV observations using a 0.6 metre telescope. A single-channel Vis Scanner photometer in a star-sky chopping mode, an S20-type photomultiplier tube, and standard Johnson UBV filters were used. Photometer control, data acquisition, and later reduction were performed using a PDP/11 computer.

(6) Ms. Gagné made BVRI observations during ingress and on one night during totality (in order to obtain R and I photometry of the secondary star) at the Climenhaga Observatory at the University of Victoria. A pulse-counting photometer at the Cassegrain focus of a

0.5 metre Lorenz reflector was used. The EMI 9658R photomultiplier was cooled with dry ice. The photometer operates under control by a Commodore 64 microcomputer, with data storage on a magnetic diskette. The observations were transferred to the VAX and reduced by the author.

Photopolarimetric observations of RZ Ophiuchi were obtained by Dr. James C. Kemp, Mr. Daniel J. Kraus, and Mr. Gary D. Henson, using the 0.6 metre reflector at Pine Mountain. Details of the equipment and observing procedures are given by Kemp and Barbour (1981). These observations are to be discussed elsewhere.

CHAPTER 3. PHOTOMETRIC ANALYSIS OF THE SYSTEM

3.1 RESULTS OF THE PHOTOMETRY

After the reductions of the photometry to the UBVRI system the data from individual observers were combined into normal points. Each normal point is the mean of typically 5 to 10 individual observations, with a quoted uncertainty from the r.m.s. standard deviation (n-1 weighting) of the distribution. These data for the light curves in U, B, and V are found in Appendix I. The light curves produced are figures 5, 6, and 7. Note that some points near θ = 7.0° and 8.2° (Australian observations) appear to be incorrect. This is probably due to the very poor weather which was encountered during some nights. It was found that the light curves were symmetric about the time of mid-eclipse predicted by Forbes and Scarfe; the light curves have thus been "folded" about phase zero to improve the coverage of the eclipse.

Numerous observations of the comparison and check stars permitted the accurate determination of their mean magnitudes and colours. These are found in table 5. The colours of the comparison and check stars correspond to those of unreddened giants of spectral type G0 and K3 respectively (Johnson, 1966), in good agreement with Forbes and Scarfe and Olson and Hickey. The R and I magnitudes used in this study are in the system defined by Cousins (1976), except for those indicated to be in the Johnson RI system (Johnson et al., 1966) by the subscript J. To be compared with tabulated values in the Johnson system the former must

FIGURE 5: ECLIPSE LIGHT CURVE IN U

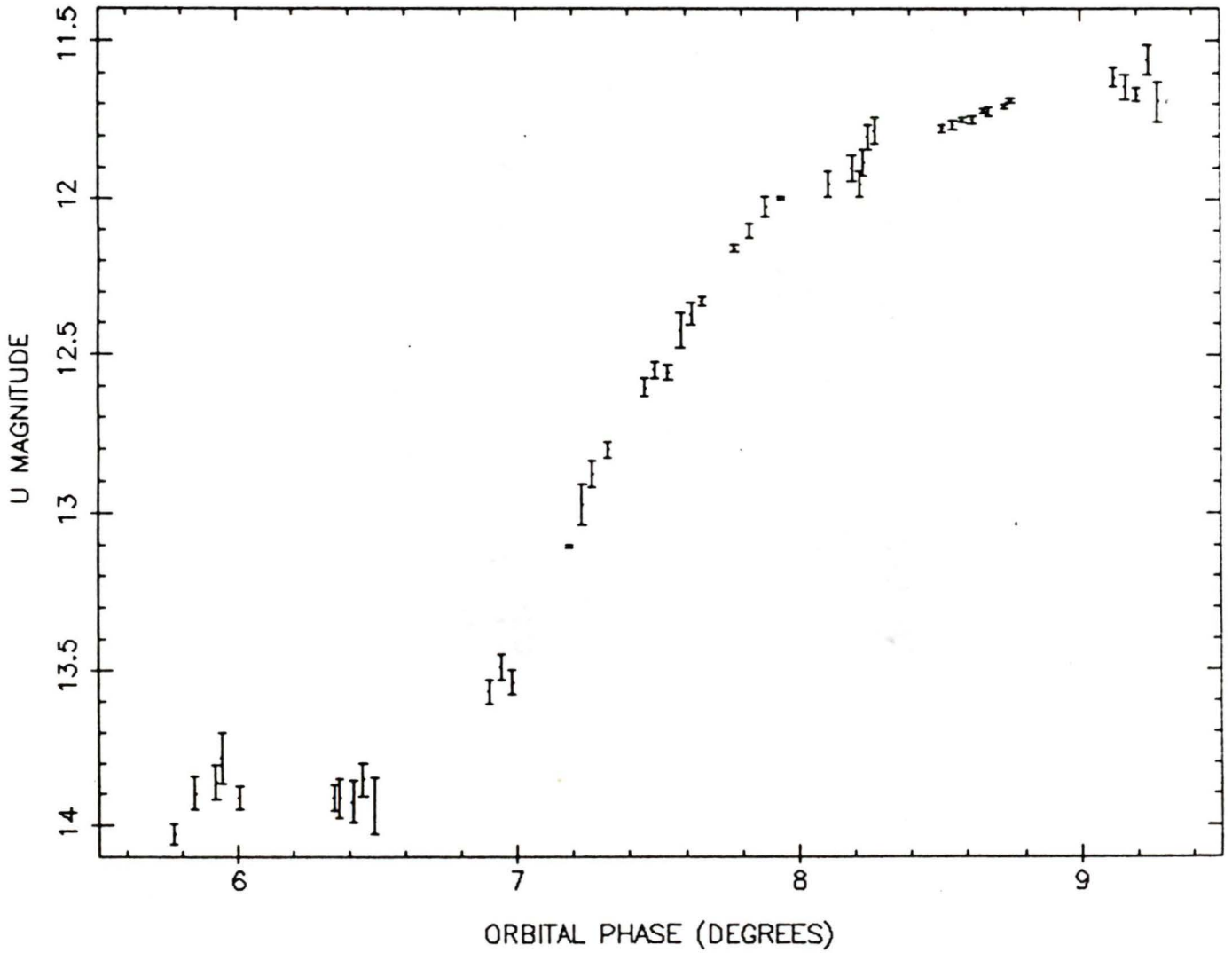

FIGURE 6: ECLIPSE LIGHT CURVE IN B

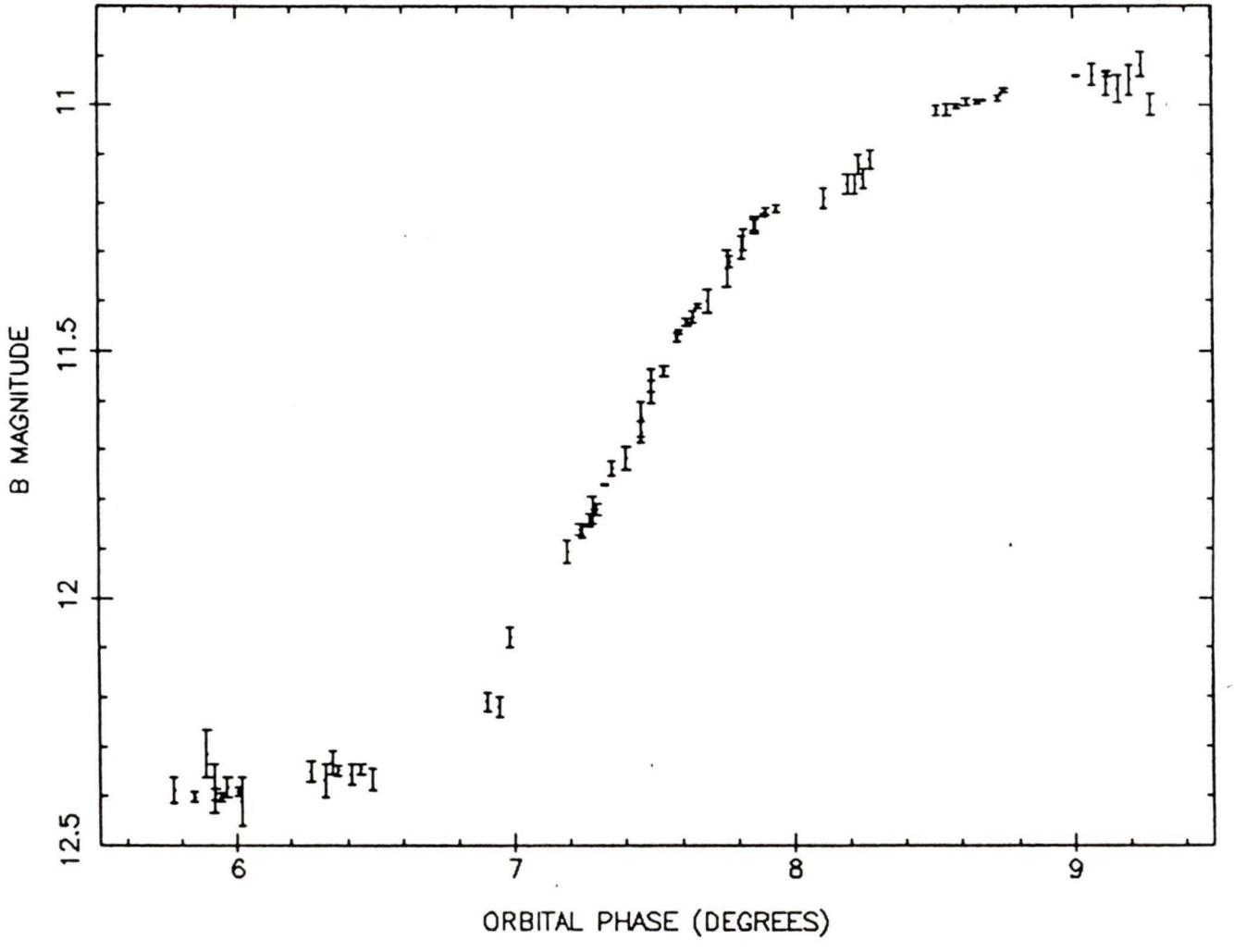

FIGURE 7: ECLIPSE LIGHT CURVE IN V

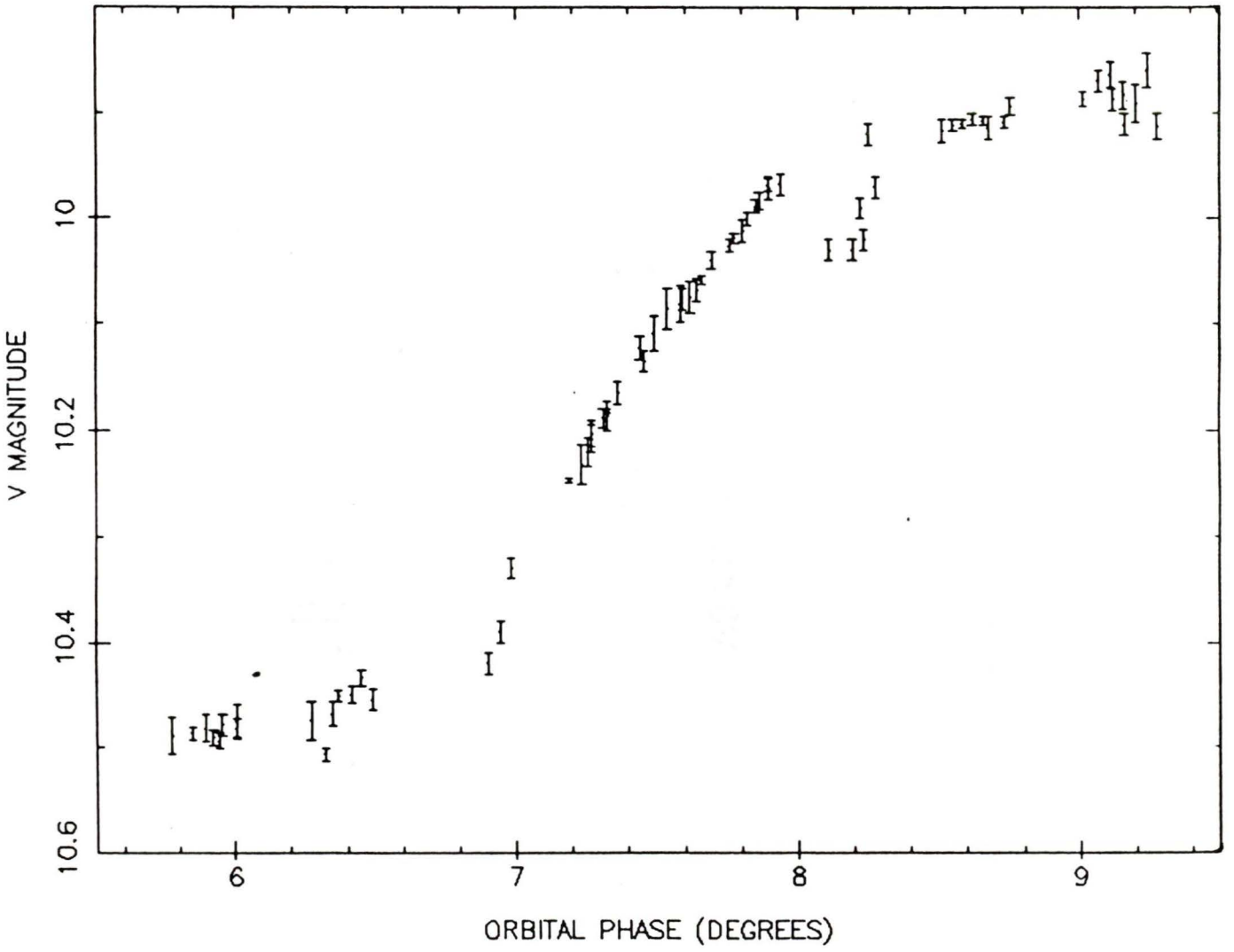

TABLE 5: MAGNITUDES AND COLOURS OF COMPARISON AND CHECK STARS

STAR	V	U-B	B-V	V-R	R-I
COMPARISON	9.412	+0.261	+0.659	+0.341	+0.254
STAR	± 0.001	± 0.002	± 0.001	± 0.004	± 0.007
CHECK	9.272	+1.266	+1.253	+0.650	+0.505
STAR	± 0.001	± 0.002	± 0.001	± 0.006	± 0.019

be transformed using the relations of Landolt (1983) or Taylor (1984).

The corresponding colour determinations for the components of RZ Ophiuchi are not as straightforward. The out-of-eclipse light curve studied by Olson and Hickey was found to vary by 0.075 magnitudes in V. The variations appear not to be symmetric in phase and to change from cycle to cycle. Olson and Hickey interpreted the variations as being due to light from the hot primary star passing through the nonuniform disk. There are also some indications of variability during totality amounting to 0.025 magnitudes in V (Olson). An attempt to apply a simple rectification (Merrill, 1963) to "flatten" the light curves proved unsuccessful (rectification will be discussed below). Much further study of the brightness variations and the disk will be necessary to account fully for these details in the light curve.

The out-of-eclipse variations occur on a timescale comparable to the orbital period; hence they should be negligible during the short period of time corresponding to the stellar eclipse. In addition, a substantial fraction of the disk is in eclipse during totality, so its contribution to the light during totality is reduced. An approximate calculation using the estimates of the disk brightness (relative to the primary star) of Olson and Hickey indicated that the contaminating effect of the disk light on the derived stellar colours would be small: the "corrected" primary F-type star colours would be bluer in U-B and B-V by about 0.05 magnitudes and the secondary K-type star colours redder by about 0.3 magnitudes in U-B and 0.2 magnitudes in B-V. These are very conservative upper limits to the colour corrections since the

calculation assumed that fully half of the disk light is visible during totality. Since the brighter innermost regions of the disk are eclipsed by the secondary star during totality, the amount of contaminating disk light will be smaller and so the colour corrections will also be smaller. Thus the depth of the eclipse in each colour and the relative brightness of each component can be determined with some confidence if the measurements are made just outside the contacts and during totality. The eclipse depths can be found by subtracting the mean magnitudes in totality from means taken just outside the contacts. Outside eclipse both stars are visible and subtraction of the relative fluxes results in the magnitudes and colours of the primary star. The magnitudes, colours, and eclipse depths calculated using this approach are found in table 6. Note that the out-of-eclipse RI photometry was performed a significant fraction of an orbital cycle later, so the V-R and R-I colours derived for the primary star may not be as reliable as the quoted uncertainties.

The U-B and B-V colours of the two components were corrected for reddening using the standard relations (Mihalas and Binney, 1981) and Olson and Hickey's value of the visual absorption of $A_V = 0.40$. The reddening corrections for the V-R and R-I colours were estimated from the relations given by Taylor. The reddening corrections and the unreddened colours appear in table 7. The unreddened colours of the two components compare well to the colours expected from their spectral types (determined by Baldwin) of F5 Ib for the primary star and K5 Ib for the secondary star (see Fernie, 1983), with the exception of the very uncertain R-I colour of the primary. As mentioned above, the

TABLE 6: OBSERVED PHOTOMETRIC PARAMETERS FOR RZ OPHIUCHI

	OUTSIDE ECLIPSE (BOTH STARS)	TOTALITY (SECONDARY STAR)	PRIMARY STAR (DERIVED)	ECLIPSE DEPTH
U	11.725 ± 0.010	14.027 ± 0.017	11.864 ± 0.012	2.302 ± 0.020
B	10.990 ± 0.003	12.392 ± 0.002	11.339 ± 0.004	1.402 ± 0.004
V	9.900 ± 0.004	10.481 ± 0.002	10.856 ± 0.010	0.581 ± 0.004
R	9.106 ± 0.006	9.439 ± 0.006	10.551 ± 0.028	0.333 ± 0.008
I	8.391 ± 0.009	8.515 ± 0.013	10.808 ± 0.136	0.124 ± 0.016
U-B	+0.735 ± 0.010	+1.635 ± 0.017	+0.525 ± 0.013	
B-V	+1.090 ± 0.005	+1.911 ± 0.003	+0.483 ± 0.011	
V-R	+0.794 ± 0.007	+1.042 ± 0.006	+0.305 ± 0.030	
R-I	+0.715 ± 0.007	+0.924 ± 0.011	-0.257 ± 0.139	

TABLE 7: REDDENING CORRECTIONS AND UNREDDENED COLOURS OF THE COMPONENTS

	REDDENING CORRECTION	SECONDARY STAR	PRIMARY STAR
U-B	0.091 ± 0.023	+1.544 ± 0.029	+0.434 ± 0.026
B-V	0.125 ± 0.032	+1.786 ± 0.032	+0.358 ± 0.034
V-R	0.085 ± 0.044	+0.957 ± 0.044	+0.220 ± 0.053
R-I	0.088 ± 0.044	+0.836 ± 0.045	-0.345 ± 0.146

TABLE 8: RESULTS OF THE T_{eff} AND BOLOMETRIC CORRECTION CALIBRATIONS

COMPONENT	T_{eff} (KELVIN)	BC (MAGNITUDES)	k
PRIMARY	6600 ± 250	+0.15 ± 0.04	
			0.13 ± 0.03
SECONDARY	3600 ± 200	-1.26 ± 0.33	

correction for disk light of the colours of the secondary are uncertain but probably small. Using the estimated upper limits to these corrections the colours of the secondary would no longer be consistent with the spectral type (particularly in B-V). The "corrected colours" of the primary star are not significantly different from those derived here. For these reasons, no corrections were applied to the colours of either component.

3.2 THE DETERMINATION OF THE RATIO OF STELLAR RADII

In the analysis of the light curves of eclipsing systems the ratio of the stellar radii k (the radius of the smaller star r_s divided by the radius of the larger star r_g) is usually a result of the analysis, in addition to the inclination i (in degrees), r_g, and the relative luminosities of the stars. In the case of RZ Ophiuchi the light curve solutions are nearly degenerate with respect to k (as found by Forbes and Scarfe and confirmed by the author in the course of this study), and so no reliable value of k can be obtained in this way. Thus an alternate procedure of obtaining a "theoretical" k through the determination of the effective temperatures and bolometric corrections of both stars was followed.

The effective temperature of a star T_{eff} is defined as the temperature that a black body radiator would have if it had the same radius and total luminosity as the star, and is given by:

$$L_\star = 4\pi R_\star^2 \, \sigma T_{eff}^4 \qquad (23)$$

where $L_\star$ is the luminosity of the star, $R_\star$ its radius, and σ is the Stefan-Boltzmann constant. $L_\star$ is measured by the absolute bolometric magnitude M_{BOL}:

$$M_{BOL} = M_V + BC = C - 2.5 \log L_\star \qquad (24)$$

where M_V is the absolute visual magnitude, BC is the bolometric correction, and C is an arbitrary constant. The bolometric correction is the difference between the absolute magnitude corresponding to the energy output over all wavelengths and the absolute magnitude measured in the V band. Using equations 23 and 24 for each star, k can be expressed as:

$$M_{BOL}(K) - M_{BOL}(F) = 10 \log (T_{eff}(F)/T_{eff}(K)) + 5 \log k \qquad (25)$$

Since the difference in the apparent magnitudes of the two stars is equal to the difference in their absolute magnitudes, we obtain:

$$M_{BOL}(K) - M_{BOL}(F) = M_V(K) + BC(K) - M_V(F) - BC(F) \qquad (26)$$

Using equations 25 and 26 a value of k can be found.

Tables of effective temperatures and bolometric corrections as a function of various colour indices are available in the literature; in the case of supergiant stars (particularly for late-type stars) these calibrations are still scarce and uncertain. The tabulations of bolometric corrections used in this study have been scaled to BC = 0.0 for the Sun.

3.2.1 THE PRIMARY STAR

For the F star calibration of T_{eff} and BC versus B-V and V-R were

done using tables from Kurucz's (1979, 1984) model atmosphere calculations of stars with solar compositions (Kurucz's tables are consistent with those of Böhm-Vitense (1981) and Flower (1977)). U-B is a poor T_{eff} indicator for stars as cool as F stars, and the R-I colour of the primary is very uncertain and not consistent with the spectral type, so these colours were not used in the calibration.

Using the results of the Strömgren photometry of Olson and Hickey, the c_1 index of the primary is +1.4 ± 0.2 and the b-y colour is +0.34 ± 0.01. c_1 is a measure of the height of the Balmer discontinuity and hence is a gravity-sensitive index at a given effective temperature, while b-y is a temperature indicator. Using the relationship between c_1, b-y, and M_V given by Strömgren (1963), an absolute magnitude of M_V = -8.1 is "predicted" for this component. This value of M_V is typical of supergiants (Allen, 1973), suggesting that the calibration of T_{eff} and BC be done assuming a low surface gravity in the atmospheric models. Baldwin's spectral classification of F5 Ib for the primary supports this idea. His classification was done in the blue region of the spectrum (which is dominated by the primary) and so should be reliable. The disk contributes mostly continuum light with some emission lines. Its presence should not significantly affect the luminosity classification of the primary. The surface gravity of a typical F5 supergiant is about log g = 1.6 (Allen).

Plots of T_{eff} versus B-V and of T_{eff} versus V-R for values of log g between 1.0 and 2.5 were made. For this range of gravity, the B-V colour of the primary indicates a temperature between 6500 K and 6700 K. This

was assumed to be the "best-bet" temperature range. Allowing for the uncertainty in the B-V colour, a temperature within the limits of 6400 K and 6900 K is indicated. This was assumed to be the "worst-case" range. Following the same procedure with the T_{eff} versus V-R plot, a best-bet range of 6500 K to 6700 K and a worst-case range of 6200 K to 7100 K were found. Comparing the two best-bet ranges, a "best-estimate" of T_{eff} = 6600 K ± 100 K is found. Using the more restrictive of the two worst-case ranges, a larger uncertainty of ± 250 K is suggested. Interpolation in the B-V versus T_{eff} tables for cool supergiants of Böhm-Vitense, a value of 6550 K is obtained, consistent with the above value.

Plotting BC versus T_{eff} over the same range of log g used above, it was found that T_{eff} = 6600 K ± 100 K corresponds to a bolometric correction BC = +0.15 ± 0.03. If the uncertainty in T_{eff} is ± 250 K, the uncertainty in BC increases to ± 0.04. Flower gives the bolometric correction of a supergiant with T_{eff} = 6600 K to be about +0.17, which is somewhat higher than the above result, but within the quoted uncertainties. To be conservative, the worst-case values of T_{eff} = 6600 K ± 250 K and BC = +0.15 ± 0.04 are adopted for the primary.

3.2.2 THE SECONDARY STAR

The secondary star is classified as a supergiant star with colours corresponding to a spectral type of K or early M. Baldwin's classification of K5 Ib was arrived at by spectroscopic observations

during totality. The only contaminating light would have been from the disk, but again disk light would not be expected to affect the luminosity classification. In addition the secondary is of lower mass but greater size than the primary, so it may be expected to have an effective temperature and bolometric correction corresponding to its luminosity class. The secondary is too cool for the Kurucz model atmospheres used above. Since the majority of the energy output of very cool (and hence very red) stars lies longward of the V band, U-B and B-V colours are poor temperature indicators. Infrared colours are much more reliable in the determination of effective temperatures and bolometric corrections of these stars, but tabulations of T_{eff} and BC versus infrared colours are difficult to come by for cool supergiants. The tables of Johnson are used here.

Before using the observed V-R and R-I colours in a temperature calibration, it will be necessary to transform them into the Johnson VRI system (as mentioned previously). Application of the transformations given by Landolt (1983) and Taylor results in $V-R_J = +1.380 \pm 0.061$ and $R-I_J = +0.189 \pm 0.052$. Interpolating T_{eff} against $V-R_J$ and $V-I_J$ gives $T_{eff} = 3450$ K $\pm$ 100 K and $T_{eff} = 3750$ K $\pm$ 100 K respectively. Taken together, they imply $T_{eff} = 3600$ K $\pm$ 200 K. This temperature results in a bolometric correction of -1.26 ± 0.33 using Johnson's tables. The adopted temperature and bolometric correction of each component and the value of k obtained from them using equations 25 and 26 are in table 8.

3.3 SOLUTIONS OF THE LIGHT CURVES

The interpretation of the light curves of eclipsing systems involve their comparison with models. The most complex of models are those which attempt to account for dynamical and astrophysical effects in physically realistic ways. The shapes of the two stars can be distorted by rotation and tidal interactions, and the surface brightnesses can be complicated by reflection effects (particularly if the orbit is close and eccentric), and by surface gravity variations. Models which include these effects include those of Wood (1971) and of Wilson and Devinney (1971).

The Russell model is a simple, essentially geometric model. The two stars are assumed to be similar ellipsoids with major axes aligned. Simple descriptions of the distortion, gravity brightening, and reflection effects are used to rectify the light curves, transforming the light curve to that of two spherical stars in a circular orbit with surface brightnesses affected only by limb darkening. This model may be insufficient, but more sophisticated models would not be justified or give substantially more reliable results when the light curves to be analyzed are preliminary in nature. It is hardly justifiable to analyze the light curves using a highly complex and realistic model unless one has data of very high quality. The light curves of RZ Ophiuchi have the additional complication of some contamination by disk light. The Russell technique was used in this study to obtain a few of the basic parameters of the system: the stellar radii and the orbital inclination.

The method of solution of the light curves followed the discussion by Irwin (1962). In the Russell model, the light curves are a function of at least 7 parameters:

(1) The light of the larger star L_g and of the smaller star L_s in terms of the total light of the system.
(2) The radii of each star in terms of the orbital radius (usually expressed as k and r_g).
(3) The orbital inclination.
(4) The limb darkening coefficients x_g and x_s of each star.

In totally-eclipsing systems such as RZ Ophiuchi, the relative luminosities are simply determined from the eclipse depths (as above). A "theoretical" value of k has been determined. Determination of the limb darkening of the star undergoing eclipse requires light curves of very high quality as the light curves are relatively insensitive to x; its value is usually assumed in the analysis. This leaves r_g and i to be determined. An attempt to rectify the light curves failed due to the complex nature of light variations outside eclipse.

Light curve solutions were performed for the data in U, B, and V, and in each case followed the same procedure. The light curves were plotted in luminosity units rather than in magnitudes, and a freehand curve drawn through the points. From well-determined sections of the light curve, points (Θ, α) were measured, where Θ is the orbital phase in degrees at that point and α is the luminosity expressed in units of

the depth of the eclipse. Approximately 20 reliable points were measured on each light curve. For each point on the light curve Irwin shows that:

$$\sin^2\theta = A^{OC} + B^{OC}\psi(x, k, \alpha) \tag{27}$$

where $A^{OC} = \sin^2\theta$ for $\alpha = 0.6$, $B^{OC} = A^{OC} - \sin^2\theta$ for $\alpha = 0.9$, and:

$$\psi(x, k, \alpha) = (\sin^2\theta(\alpha) - A^{OC})/B^{OC} \tag{28}$$

is a function which can be calculated for any value of x, k, and α. Extensive tabulations of $\psi(x, k, \alpha)$ appear in the work of Merrill (1950). For the set of points measured on the light curve, a linear regression of $\psi(x, k, \alpha)$ (obtained by linear interpolation in Merrill's tables) versus $\sin^2\theta$ will yield least-squares values of A^{OC} and B^{OC}.

Once A^{OC} and B^{OC} are determined, r_g and i are found from:

$$\phi_1(x, k) = 4k\,(\psi(x, k, 0) - \psi(x, k, 1))^{-1} \tag{29}$$

$$\phi_2(x, k) = 4k\,((1 - k)^2\,\psi(x, k, 0) - (1 + k)^2\,\psi(x, k, 1))^{-1} \tag{30}$$

$$\cot^2 i = B^{OC}/\phi_2(x, k) - A^{OC} \tag{31}$$

$$r_g^2 \csc^2 i = B^{OC}/\phi_1(x, k) \tag{32}$$

Tables of $\phi_1(x, k)$ and $\phi_2(x, k)$ are also found in Merrill's work. Calculations of the phases of the eclipse contacts can be made using equation 27 with $\alpha = 0$ (external contact θ_e) and with $\alpha = 1$ (internal contact θ_i). Equation 27 can also be used to synthesize the light curve corresponding to the solution. The "observed" and "calculated" light curves can then be compared.

3.4 RESULTS OF THE LIGHT CURVE SOLUTIONS

The value x = 0.6 appropriate to F stars in the visual band was

assumed in the solution of the V light curve. The points on the light curve used in the solution of A^{OC} and B^{OC} are in table 9, as well as the values of A^{OC} and B^{OC} determined by least-squares. Care was taken to use only the well-determined parts of the light curve in the solution.

The correlation coefficient of the linear fit was greater than 0.999, and the calculated uncertainties of the determination of A^{OC} and B^{OC} were both of the order of 10^{-5}. The results of the solution are in table 10. The synthesized V light curve is shown in figure 8 and the table of (O-C)'s is in Appendix II. The table of (O-C)'s indicate that a satisfactory solution has been obtained. Unfortunately, the light curve solution in V (as well as in B and U) suffers from a lack of data near the contacts. Solutions are very sensitive to the light curves near the contacts, and so are important in the verification of the fit of the synthesized light curve to the data.

To obtain an estimate of the uncertainty in the solution, solutions were carried out for k = 0.10 and 0.16 (the estimated extreme values of k). The quoted uncertainties in table 10 are based on the two "extreme" solutions (except those of the luminosities and of k). The extreme values of i appear in parentheses in table 10.

The same procedure was followed in the solution of the B and U light curves. The value x = 0.8 was used in these solutions. Table 9 contains the points used in the solution for A^{OC} and B^{OC}; the fits were generally comparable in quality to that of the V data. The results of these fits also appear in table 10 and (O-C)'s in Appendix II. Figures 9 and 10 show the synthesized light curves in B and U. The fit in B is

TABLE 9: DATA USED IN LIGHT CURVE SOLUTIONS

U		B		V	
α	θ (°)	α	θ (°)	α	θ (°)
0.025	8.56	0.250	7.92	0.150	7.92
0.050	8.47	0.275	7.88	0.175	7.88
0.150	8.21	0.300	7.84	0.200	7.84
0.175	8.16	0.325	7.81	0.225	7.80
0.200	8.11	0.350	7.76	0.250	7.76
0.475	7.67	0.375	7.73	0.275	7.73
0.500	7.63	0.400	7.71	0.300	7.69
0.525	7.60	0.425	7.68	0.325	7.65
0.550	7.57	0.450	7.64	0.350	7.62
0.600	7.51	0.475	7.61	0.375	7.58
0.625	7.47	0.500	7.58	0.400	7.54
0.650	7.44	0.525	7.55	0.425	7.51
0.700	7.36	0.550	7.52	0.450	7.47
0.725	7.32	0.575	7.49	0.475	7.43
0.750	7.28	0.600	7.46	0.500	7.40
0.775	7.24	0.625	7.43	0.525	7.36
0.800	7.20	0.650	7.40	0.550	7.32
0.825	7.16	0.675	7.38	0.575	7.29
		0.700	7.33	0.600	7.26

TABLE 9: (CONTINUED)

U		B		V	
α	Θ (°)	α	Θ (°)	α	Θ (°)
		0.725	7.29	0.625	7.23
		0.750	7.24	0.650	7.20
		0.775	7.20		
$A^{OC} = 0.0171$		$A^{OC} = 0.0168$		$A^{OC} = 0.0160$	
$B^{OC} = 0.00223$		$B^{OC} = 0.00191$		$B^{OC} = 0.00200$	

TABLE 10: LIGHT CURVE SOLUTIONS

	U	B	V
L_g	0.120 ± 0.002	0.275 ± 0.001	0.586 ± 0.003
L_s	0.880 ± 0.002	0.725 ± 0.001	0.414 ± 0.003
k	0.13 ± 0.03	0.13 ± 0.03	0.13 ± 0.03
x (ASSUMED)	0.8	0.8	0.6
Θ_e (°)	8.721 ± 0.010	8.511 ± 0.016	8.375 ± 0.011
Θ_i (°)	6.618 ± 0.026	6.696 ± 0.018	6.466 ± 0.026
i (°)	88.3	90.0	90.0
RANGE OF i (°)	(85.4, 90.0)	(86.7, 90.0)	(86.0, 90.0)
r_g	0.137 ± 0.016	0.127 ± 0.015	0.128 ± 0.016
r_s	0.018 ± 0.002	0.017 ± 0.002	0.017 ± 0.002

FIGURE 8: V LIGHT CURVE SOLUTION

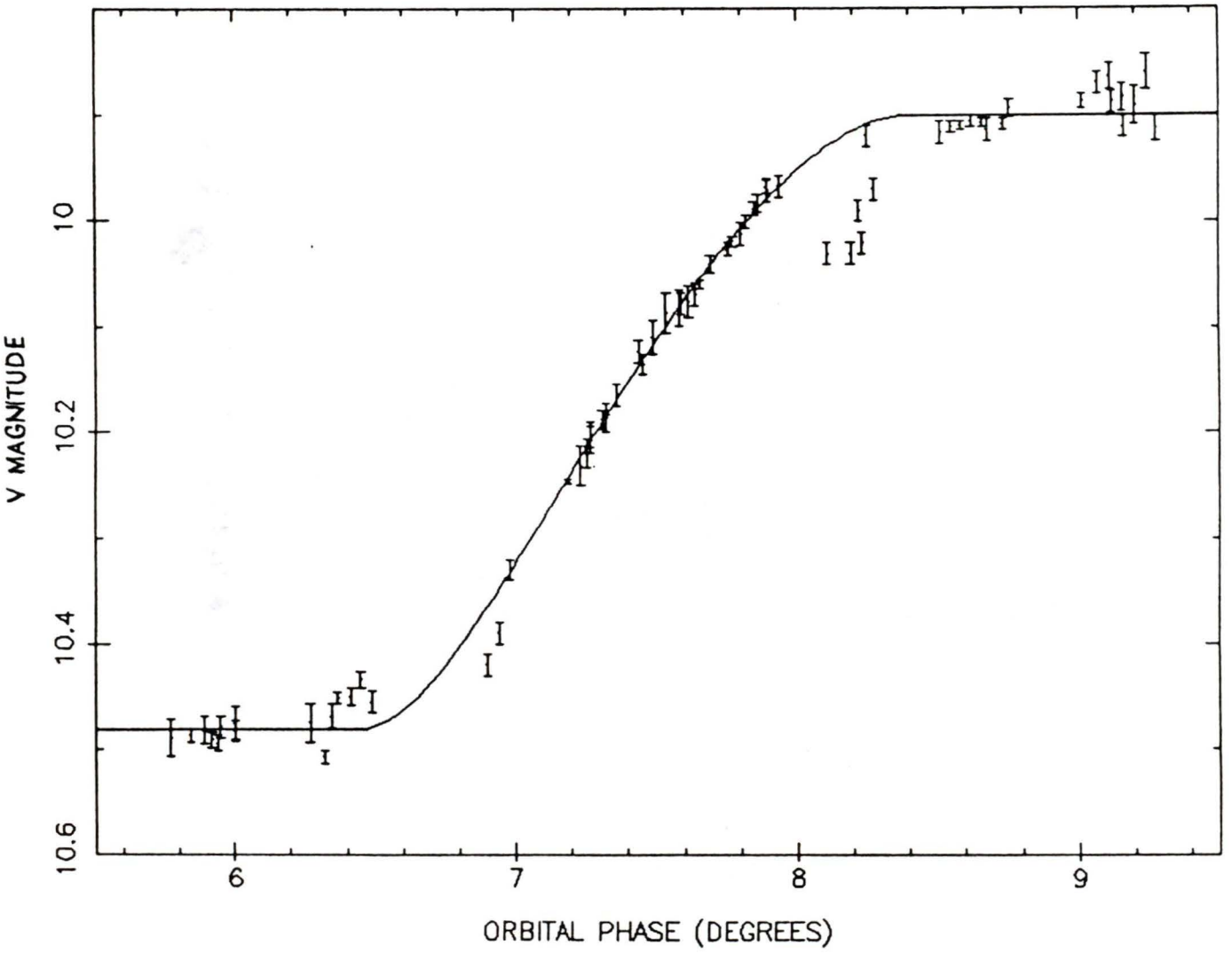

FIGURE 9: B LIGHT CURVE SOLUTION

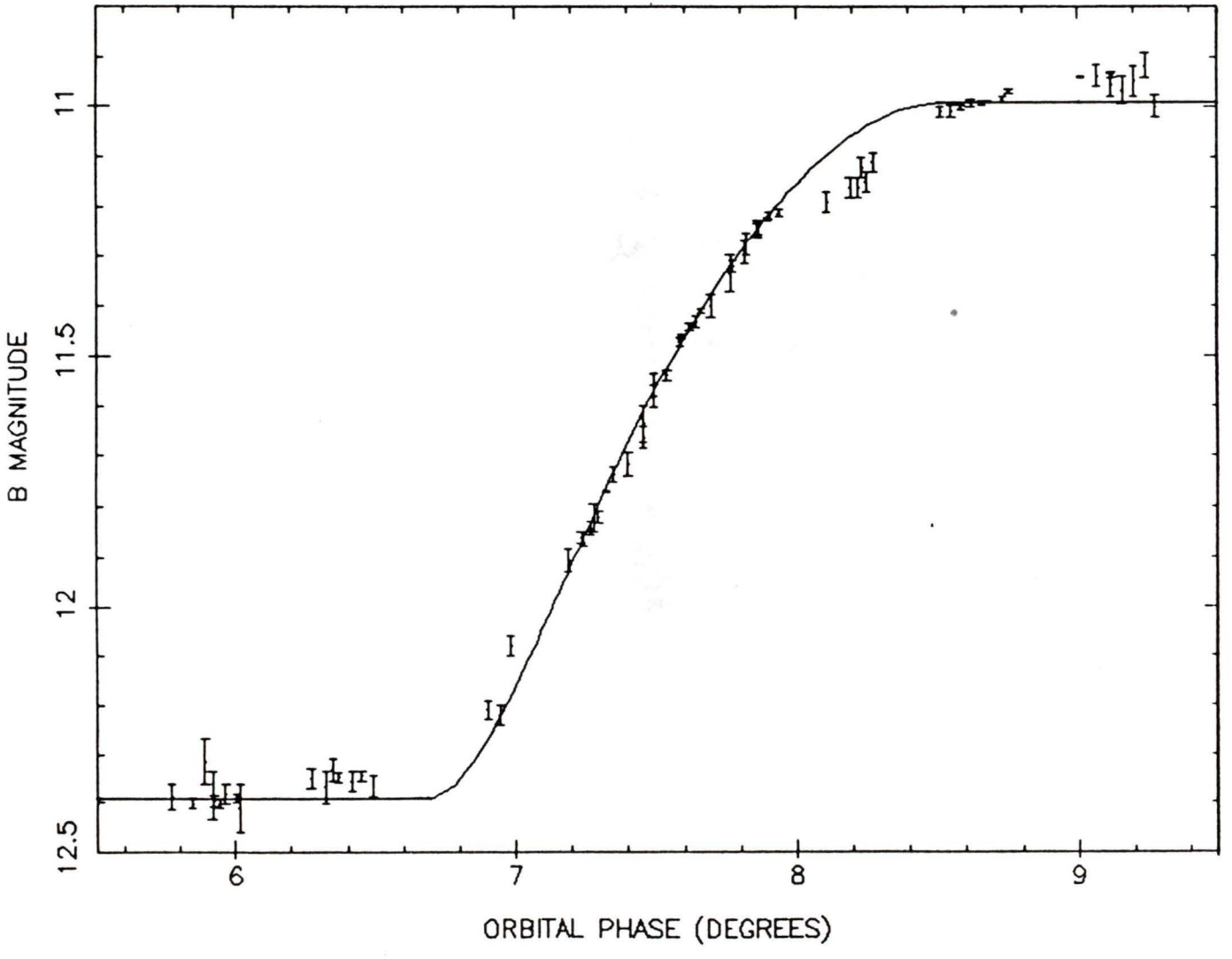

FIGURE 10: U LIGHT CURVE SOLUTION

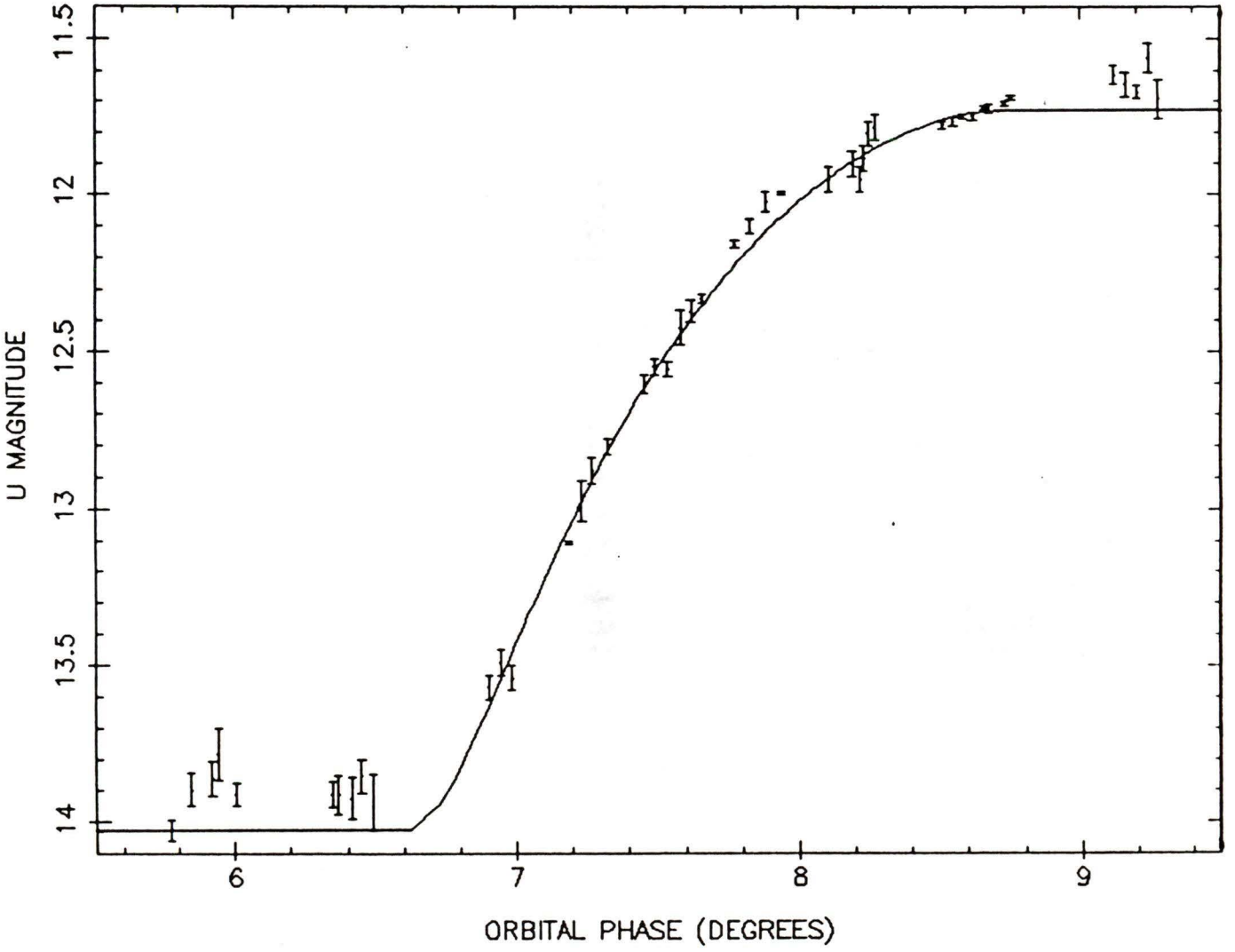

quite good but is less so in U. This is likely due to the faintness of RZ Ophiuchi in U during the eclipse phases. The magnitudes at mid-eclipse used in the solutions are means taken throughout totality. There appears to be some variation in U during totality and as a result the U light curve appears to lie somewhat above the mean level near internal contact.

The values of i, r_g, and r_s adopted for following discussions are $i = 90.0° \pm 4.0°$, $r_g = 0.13 \pm 0.02$, and $r_s = 0.017 \pm 0.002$.

CHAPTER 4. MODEL OF RZ OPHIUCHI

4.1 DIMENSIONS AND MASS OF THE SYSTEM

Little further progress can be made in determining the physical parameters of the system without the radial-velocity information obtained from spectroscopy. Baldwin's original radial-velocity study was preliminary in nature. Fortunately, a new spectroscopic orbital solution for the RZ Ophiuchi system has been made available by Dr. Michel Mayor of the Observatoire de Geneve. The spectroscopic observations were performed by the CORAVEL radial-velocity scanner (Baranne et al., 1979) at the Haute-Provence Observatory during the period 1977-1984. The CORAVEL observations appear in table 11, the radial-velocity curves in figure 11, and the results of the spectroscopic solution are given in table 12. There, e is the orbital eccentricity, γ the systemic (centre-of-mass) radial-velocity, T_0 the time of nodal passage of the primary, and K_1 and K_2 are the radial-velocity semi-amplitudes of each star (the subscripts 1 and 2 will refer to the primary and the secondary respectively in the following discussions and the subscript $\odot$ will indicate that the quantity is expressed in terms of the Sun). Recent observations obtained by Scarfe (table 13) using the radial-velocity scanner at the Dominion Astrophysical Observatory (Fletcher et al., 1982) are consistent with the radial velocity curves of Mayor (see figure 11).

TABLE 11: CORAVEL RADIAL-VELOCITY OBSERVATIONS

JD - 2 440 000	V_r(PRI) (km/s)	JD - 2 440 000	V_r(SEC) (km/s)
3698.458	+5.0 ± 0.7	3401.301	-25.9 ± 1.2
3699.508	+5.9 ± 1.3	3696.493	-53.1 ± 0.8
3711.417	+6.8 ± 1.4	3699.496	-53.8 ± 0.7
3720.437	+6.1 ± 1.3	3700.485	-53.8 ± 1.0
3730.438	+4.1 ± 1.1	3711.410	-54.6 ± 1.0
3733.361	+5.6 ± 2.3	3720.432	-55.8 ± 0.9
4100.406	-11.2 ± 2.3	3730.429	-51.2 ± 1.4
4113.361	-4.7 ± 1.8	4100.388	+53.7 ± 1.0
5582.364	+1.0 ± 1.7	4113.355	+51.9 ± 1.3
5582.373	-1.6 ± 2.0	4407.535	+25.3 ± 1.1
5916.397	-4.3 ± 1.8	5171.487	+50.7 ± 1.1
5916.406	-7.3 ± 1.4	5193.386	+26.2 ± 0.7
5942.400	-8.8 ± 1.3	5193.395	+25.9 ± 0.8
		5582.364	-33.5 ± 1.3
		5582.373	-33.5 ± 1.1
		5916.397	+47.5 ± 1.4
		5942.387	+54.3 ± 0.9

FIGURE 11: RADIAL–VELOCITY CURVES OF RZ OPHIUCHI

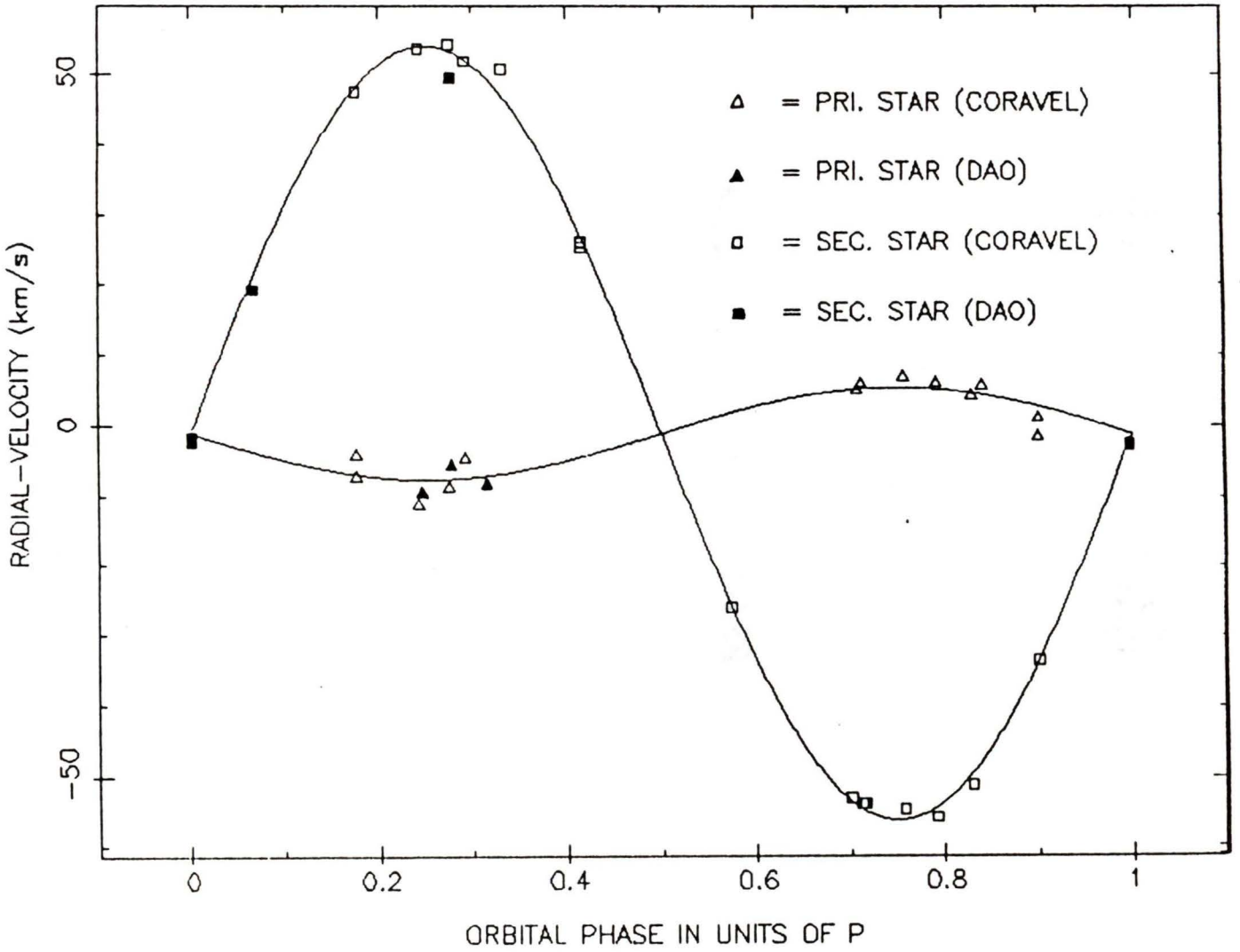

TABLE 12: CORAVEL RADIAL-VELOCITY SOLUTION

P (DAYS)	261.9277	(BALDWIN)
e	0.0	(IMPOSED)
T_0 (JD - 2 440 000)	4102.4 ± 0.4	
γ (km/s)	-1.1 ± 0.3	
K_1 (km/s)	6.5 ± 0.6	
K_2 (km/s)	55.1 ± 0.5	

TABLE 13: D. A. O. RADIAL-VELOCITY OBSERVATIONS

JD - 2 440 000	V_r(PRI) (km/s)	JD - 2 440 000	V_r(SEC) (km/s)
5934.816	-9.55 ± 1.15	5869.813	-2.75 ± 0.19
5952.708	-8.22 ± 1.85	5869.856	-2.50 ± 0.24
5952.745	-8.27 ± 0.68	5870.779	-2.44 ± 1.03
6204.936	-5.73 ± 1.40	5870.820	-1.75 ± 0.20
		5887.827	+19.29 ± 0.65
		6204.936	+49.55 ± 0.51

The semi-major axis of the orbit of each component around the centre of mass follow from:

$$K = na \sin i/(1 - e^2)^{1/2} \qquad (33)$$

where $n = 2\pi/P$. Using this equation, $a_1 = 34\ R_\odot \pm 3\ R_\odot$ and $a_2 = 285\ R_\odot \pm 3\ R_\odot$. The separation of the components is thus $a = a_1 + a_2 = 319\ R_\odot \pm 4\ R_\odot$. Assuming that the disk eclipse has a duration of about 42 days, its radius is approximately $110\ R_\odot$.

The total mass of the system is given by Kepler's Third Law (in solar units):

$$M_1 + M_2 = a^3/P^2 \qquad (34)$$

This gives a total mass of $6.3\ M_\odot \pm 0.2\ M_\odot$.

4.2 PHYSICAL CHARACTERISTICS OF THE STARS

The value of a and the values of r_g and r_s determined from the photometry allows the determination of the absolute radii of the stars: $R_1 = 5.4\ R_\odot \pm 0.6\ R_\odot$ and $R_2 = 41\ R_\odot \pm 6\ R_\odot$.

It can be seen immediately that the mass ratio of the two stars $M_1/M_2 = K_2/K_1 = 8.5 \pm 0.6$ is much larger than the value 2.67 found by Baldwin. Baldwin's radial-velocity survey used plates taken at the relatively low reciprocal dispersions of 15 Å/mm and 30 Å/mm (the radial-velocity scanner at the DAO has a reciprocal dispersion of 2.4 Å/mm). Baldwin cites the blending of lines of the primary and the secondary as a possible problem. Other problems might be caused by the poor phase coverage of the radial-velocity curves or the fact that the

radial-velocity curve of the secondary was based on measurements of only one line.

Combining the value of the total mass of the system with the mass ratio, the masses of the stars are $M_1 = 5.7\ M_\odot \pm 0.2\ M_\odot$ and $M_2 = 0.7\ M_\odot \pm 0.1\ M_\odot$.

Once the mass and radius of a star is determined, the value of the surface gravity can be calculated using:

$$\log g_\star = \log g_\odot + \log M_\star - 2 \log R_\star \qquad (35)$$

where $\log g_\odot = 4.44$ (log cm/s^2) and $M_\star$ and $R_\star$ are expressed in solar units. The surface gravities of the two components are $\log g_1 = 3.7 \pm 0.1$ and $\log g_2 = 1.0 \pm 0.1$.

The mass, radius, and gravity of the primary star are those typical of an F5 giant star (Allen, 1973, Mihalas and Binney). Using the values of the effective temperature, radius, and bolometric correction of the primary, its absolute bolometric magnitude is $M_{BOL} = +0.5 \pm 0.2$ and its absolute visual magnitude is $M_V = +0.3 \pm 0.2$. These values correspond to an F5 II-III star. Using the approximate formula of Eggleton (1983), the critical radius of the primary is $180\ R_\odot \pm 3\ R_\odot$. The primary is well within its critical lobe (the radius of the disk surrounding the primary is 60% of the critical radius).

In summary, the physical characteristics of the primary appear to be those of a normal F5 II-III star, with the exception of its supergiant-like spectrum.

The secondary star is a very unusual object. It has the radius of a K5 giant, a surface gravity approaching that of a supergiant, but the

mass of only a dwarf K star. The values of T_{eff}, $R_{\star}$, and BC for the secondary result in $M_{BOL} = -1.3 \pm 0.4$ and $M_V = 0.0 \pm 0.5$, values typical for a K5 III star. The size of the critical Roche lobe is 69 $R_{\odot} \pm 2\ R_{\odot}$, using Eggleton's formula. Thus the secondary star also does not fill its critical surface, having a radius only 60% of the critical radius. RZ Ophiuchi is therefore a detached system (and lies some 1100 pc ± 200 pc from the Sun, based upon the absolute magnitudes of the two components).

It should be noted that the surface gravity of the primary star is outside the range of surface gravities used in the determination of its effective temperature and bolometric correction. If instead the primary has the effective temperature and bolometric correction of a giant star, this will affect the determination of k. A giant with the colours of the primary will have an effective temperature of about 6850 K and a BC of +0.10 (using the tables of Kurucz for a value of log g = 3.5). The ratio of the radii is then found to be 0.12. This value of k is not significantly different from the value of $k = 0.13 \pm 0.03$ determined earlier.

4.3 DISCUSSION OF THE EVOLUTIONARY HISTORY OF RZ OPHIUCHI

The present state of the RZ Ophiuchi system is almost certainly a result of the transfer of substantial amounts of matter from the originally more massive star (now the less massive secondary) to the other, less massive star (now the more massive primary), as evidenced by the peculiar properties of the secondary and the circumstellar disk of

the primary. It is also possible that a significant amount of mass was lost from the system as a whole.

Mass exchange in close binaries can begin during one of three different phases in the evolution of the mass-losing star (Trimble, 1983). Case A mass transfer occurs when the expansion of the mass-loser during Main Sequence core hydrogen-burning causes it to overflow its critical surface. Case B mass transfer occurs after core hydrogen exhaustion, following which the core contracts and the outer regions of the star expand, resulting in a red giant star. Case C mass exchange can occur in stars more evolved than the core helium-burning stage. As in Case B, the outer layers expand to overflow the critical surface, in this case after core helium-burning has finished.

Which type of mass transfer occurs in a system depends on the original mass ratio and the separation as they determine the Roche lobe sizes. Assuming that no mass or orbital angular momentum is lost from the system during mass transfer ("the conservative case"; most calculations of the evolution of close binaries adopt these assumptions), lower limits can be set to the original mass of the mass-loser and the orbital separation. In the conservative case, the minimum separation occurs when both stars are of equal mass. In the case of RZ Ophiuchi, if $M_1 = M_2 = 3.2\ M_\odot$, this minimum separation is $a = 48\ R_\odot$. Since the mass-loser initially must be the more massive component in order that its evolution proceed faster than the other component, the initial separation must be greater than $48\ R_\odot$. The minimum Roche radius of the mass-loser also occurs near a mass ratio of

unity, and is found to be roughly 20 $R_\odot$.

The Main Sequence radius of a star of mass 6.3 $M_\odot$ is only 4 $R_\odot$ (Mihalas and Binney). Since the mass-loser was obviously less massive and so had a Main Sequence radius less than 4 $R_\odot$, the possibility of Case A mass transfer is ruled out.

Case B mass transfer is certainly possible given that red giant radii can be much greater than the minimum Roche radius of 20 $R_\odot$ found above. Two possible evolutionary scenarios for Case B have been proposed which depend on the original mass of the mass-loser.

Kippenhahn and Weigert (1967) have shown that if the mass-loser had a mass greater than about 3 $M_\odot$ then mass transfer would be terminated by the onset of core helium-burning. By this time the outer envelope of the mass-loser has been almost completely stripped of hydrogen, and the star may look like a helium star or (if the star was substantially more massive than 3 $M_\odot$) a Wolf-Rayet star (Kippenhahn, 1969). Models of intermediate mass close binaries (systems with a total mass between 3 $M_\odot$ and 15 $M_\odot$) undergoing Case B mass transfer tend to produce a bright Main Sequence B-type star (the mass-gainer) and a much fainter helium star (the mass-loser) (van der Linden, 1980).

If the mass-loser was originally less massive than about 3 $M_\odot$, contraction of the helium core will be halted by degeneracy. Shell hydrogen-burning continues outside the core. When this burning has exhausted most of the remaining hydrogen, the outer layers of the star will contract away from the Roche surface. The envelope is very rarefied and extended, and the star will look like a low mass red giant

(Paczyński, 1971). It is possible that mass loss will continue from the tenuous outer atmosphere (Paczyński, 1969). As the envelope continues to contract, the degenerate core will become visible, and the star becomes a low mass ($M_* < 0.3\ M_\odot$) white dwarf (Kippenhahn and Weigert, 1969). The time required for the contraction to the white dwarf stage is very short, approximately 10^4 years (Deinzer and Hansen, 1969).

The mass-loser in the RZ Ophiuchi system must have had a mass greater than 3.2 $M_\odot$, which would suggest that the first type of Case B evolution ought to have occured, but the present state of the system is not as expected if it did. The results of the second type of Case B evolution describe the present state of RZ Ophiuchi somewhat better, but it is quite possible that the mass-loser was initially significantly above the limit of 3 $M_\odot$. However, it is not possible to rule out this type of Case B evolution completely, particularly if the two components were originally nearly equal in mass. If so, and if the evolution of the mass-gaining star was not greatly affected by mass transfer (Shu and Lubow, 1981), the advanced evolutionary state of the mass-gainer could be explained.

Very little is known about Case C mass transfer. Few model calculations have yet been published, and the only evolutionary calculations which appear to be available for an intermediate mass system undergoing Case C mass transfer have been published by Lauterborn (1970). The starting point of his calculation was two stars of mass 5 $M_\odot$ and 2 $M_\odot$ separated by 302 $R_\odot$. The 5 $M_\odot$ star was found to overflow its Roche surface during the expansion following core helium exhaustion

and rapidly transferred 4 $M_\odot$ of matter to the other component. When the star detached from its Roche lobe, it had a mass of only 1 $M_\odot$, had a carbon-oxygen core, and was burning helium in a shell. The mass-loser never contracted to less than about 0.7 times the radius of its critical radius during this detached phase, which lasted approximately $6 \cdot 10^5$ years. The star looked like a low mass red giant with a degenerate carbon-oxygen core and a very tenous outer envelope. Eventually, hydrogen-burning began in a second shell and the mass-loser overflowed its Roche lobe for a second time. The remaining envelope was stripped from the star (or burned by the double-shell source), leaving behind a star not massive enough to burn carbon in the core. The star became a carbon-oxygen white dwarf of relatively high mass (about 1 $M_\odot$). The time required for the mass-loser to evolve from this second semi-detached phase to a white dwarf was about $4 \cdot 10^4$ years.

The parameters of the initial model in Lauterborn's work are quite plausible ones for the initial state of RZ Ophiuchi. The present appearance of this system corresponds well to the detached phase in which the mass-loser is burning only helium in a shell. It may instead be the case that RZ Ophiuchi has passed the second semi-detached phase and the mass-loser is on its way to becoming a white dwarf. However, the short time-scale of this phase makes it much less likely to be observed than the previous detached phase. The radius of the mass-loser in the first detached phase (about 0.7 times the critical radius) is very close to that for the mass-loser in the RZ Ophiuchi system (0.6 times the critical radius). In addition, the position of the secondary in the

Hertzsprung-Russell diagram is more consistent with the position of the model mass-loser during the first detached phase than with its position during the second detached phase. The existence of the circumstellar disk can more plausibly be accounted for if the secondary has recently detached from its critical surface for the first time since the vast majority of the total mass lost by this component is lost during the first semi-detached phase. Remnants of the accretion disk would more likely be observable soon after the phase of large (and rapid) mass loss than after a phase of very small (and slower) mass loss. Estimates of the mass of the disk range from approximately 10^{-9} $M_{\odot}$ (Baldwin) to 10^{-7} $M_{\odot}$ (Olson and Hickey). Since cool giants such as the secondary star lose mass through stellar winds at rates of about 10^{-6} $M_{\odot}$ per year, it is not unreasonable to suggest that the disk is still being "fed" by the secondary.

Thus, it appears that the most likely description of RZ Ophiuchi is as a system fortuitously caught between Roche lobe fillings in Case C mass transfer; this system may be an example of a short-lived phase of close binary evolution, and may indeed be unique among known binaries in this characteristic.

4.4 SUMMARY AND SUGGESTIONS FOR FURTHER RESEARCH

This thesis has presented the results of a new observational study of the eclipsing binary system RZ Ophiuchi. Light curves in three colours (U, B, and V) were obtained during the 1984 summer eclipse

through the efforts of a worldwide network of observers. The quantity of useful data acquired and the much better phase coverage make these eclipse light curves the best yet produced for this system.

Reliable values of the U-B and B-V colours of each component were obtained, along with a lesser amount of R and I photometry which permitted some infrared colours of each component to be determined. These colours (when corrected for reddening) and the spectral classifications of the components were used to derive the value of the effective temperature and bolometric correction of each star and hence the ratio of the radii k of the two stars.

Since the light curve solutions were degenerate with respect to k, the value determined through the stellar colours was used in the Russell model solutions. These solutions yielded the values of i, r_g, and r_s.

The combination of the light curve solutions with the new radial-velocity solution of Mayor allowed the dimensions of the binary orbit and the absolute radius and mass of each star to be calculated. The primary star was found to be a relatively normal F-type giant. The secondary star appears to be a low mass K-type giant. Neither star fills its critical Roche lobe.

The results of the combined photometric-spectroscopic solution support the detached model favoured by Baldwin and by Forbes and Scarfe. The semi-detached model favoured by Smak, in which the secondary fills its Roche lobe, is ruled out.

A comparison of the present state of the RZ Ophiuchi system to the results of the three major models of mass transfer suggests that RZ

Ophiuchi is an example of a Case C mass transfer binary during a short-lived phase of its evolution. It is suggested that the observed disk surrounding the primary is a remnant of the previous rapid phase of mass transfer and still may be fed by a stellar wind from the tenuous outer envelope of the secondary.

Although some progress has been made in understanding the RZ Ophiuchi system, it is clear that further investigations would be of great benefit. Among the possibilities for further observational study of the RZ Ophiuchi system are:

(1) Continued efforts to refine the light curves of primary eclipse. As mentioned earlier, the coverage of the light curves near external and internal contact is still poor.

(2) Substantially more infrared observations of the secondary star during totality to establish its effective temperature and bolometric correction more securely.

(3) Obtaining satellite far-ultraviolet spectra outside stellar eclipse. This should help determine the properties of the disk (in particular, the temperature), and also help determine to what extent it affects the appearance of the system.

(4) An abundance analysis of the secondary. This would require high dispersion, high signal-to-noise spectroscopy during totality, and would be difficult to do. However, it might be possible to detect the peculiar composition (helium enhancement) expected of a star in the last stages of evolution before appearing as a white dwarf.

It is unfortunate that RZ Ophiuchi, like many other long-period systems, has been little studied. The point should be emphasized that the long period interacting systems are those that will allow researchers to study the phenomemon of Case C systems observationally. A better understanding of this type of mass transfer holds implications for the study of long period systems containing a white dwarf star (just one example being the Sirius problem) and of the study of the late stages of stellar evolution in general.

REFERENCES

Allen, C. W., 1973. "Astrophysical Quantities", p.196. Athlone Press, London.

Baldwin, B. W., 1976. "An Observational Study of the Eclipsing Binary RZ Ophiuchi" (Ph.D. Thesis), U. of Victoria.

Baldwin, B. W., 1978. Astrophys. J., 226, 937.

Baranne, A., Mayor, M., and Poncet, J. L., 1979. Vistas in Astron., 23, 279.

Bohm-Vitense, E., 1981. Ann. Rev. Astron. Astrophys., 19, 295.

Cousins, A. W. J., 1976. Mem. R. Astron. Soc., 81, 25.

Crawford, J. A., 1955. Astrophys. J., 121, 71.

Deinzer, W., and Hansen, C. J., 1969. Astron. Astrophys., 3, 214.

Eggleton, P. P., 1983. Astrophys. J., 268, 368.

Fernie, J. D., 1983. Astrophys. J. Suppl., 52, 7.

Fletcher, J. M., Harris, H. C., McClure, R. D., and Scarfe, C. D., 1982. Publ. Astron. Soc. Pac., 94, 1017.

Flower, P. J., 1977. Astron. Astrophys., 54, 31.

Forbes, D., and Scarfe, C. D., 1984. Publ. Astron. Soc. Pac., 96, 737.

Hall, D. S., and Genet, R. M., 1982. "Photoelectric Photometry of Variable Stars". I.A.P.P.P..

Hardie, R. H., 1962. In "Astronomical Techniques", edited by W. A. Hiltner, p. 178. U. of Chicago Press, Chicago.

Henden, A. A., and Kaitchuck, R. H., 1982. "Astronomical Photometry". Van Nostrand Reinhold Co., New York.

Hiltner, W. A., 1946. Astrophys. J., 104, 400.

Irwin, J. B., 1962. In "Astronomical Techniques", edited by W. A. Hiltner, p. 584. U. of Chicago Press, Chicago.

Johnson, H. L., 1962. In "Astronomical Techniques", edited by W. A. Hiltner, p. 157. U. of Chicago Press, Chicago.

Johnson, H. L., 1966. Ann. Rev. Astron. Astrophys., 4, 193.

Johnson, H. L., Mitchell, R. I., Iriarte, B., and Wisniewski, W. Z., 1966. Comm. Lunar Planet. Lab., 4, 99.

Kemp, J. C., 1984. private communication.

Kemp, J. C., and Barbour, M. S., 1981. Publ. Astron. Soc. Pac., 93, 521.

Kippenhahn, R., 1969. Astron. Astrophys., 3, 83.

Kippenhahn, R., and Weigert, A., 1967. Z. Astrophys., 65, 251.

Kippenhahn, R., and Weigert, A., 1969. In "Low Luminosity Stars", edited by S. S. Kumar, p. 373. Gordon and Breach Science Publ., Inc., New York.

Kurucz, R. L., 1979. Astrophys. J. Suppl., 40, 1.

Kurucz, R. L., 1984. unpublished.

Lallemand, A., 1962. In "Astronomical Techniques", edited by W. A. Hiltner, p. 126. U. of Chicago Press, Chicago.

Landolt, A. U., 1973. Astron. J., 78, 959.

Landolt, A. U., 1983. Astron. J., 88, 439.

Lauterborn, D., 1970. Astron. Astrophys., 7, 150.

Merrill, J. E., 1950. Contr. Princeton U. Observ., No. 23.

Merrill, J. E., 1963. In "Photoelectric Astronomy for Amateurs", edited by F. B. Wood, p. 163. The Macmillan Co., New York.

Mihalas, D., and Binney, J., 1981. "Galactic Astronomy", p. 180. W. H. Freeman and Co., San Francisco.

Morton, D. C., 1960. Astrophys. J., 132, 146.

Olson, E. C., 1984. private communication.

Olson, E. C., and Hickey, J. P., 1983. Astrophys. J., 264, 251.

Paczyński, B., 1969. Acta Astron., 19, 1.

Paczyński, B., 1971. Ann. Rev. Astron. Astrophys., 9, 183.

Plavec, M. J., 1980. In "Close Binary Stars: Observations and Interpretation", edited by M. J. Plavec, D. M. Popper, and R. K. Ulrich, p. 251. D. Reidel Publ. Co., Dordrecht.

Seares, F. H., 1908. Laws Obs. Bull., No. 16.

Shu, F. H., and Lubow, S. H., 1981. Ann. Rev. Astron. Astrophys., 19, 277.

Smak, J., 1981. Acta Astron., 31, 25.

Strömgren, B., 1963. In "Basic Astronomical Data", edited by K. Aa. Strand, p. 123. U. of Chicago Press, Chicago.

Taylor, B. J., 1984. preprint.

Trimble, V., 1983. Nature, 303, 137.

van der Linden, Th. J., 1980. In "Close Binary Stars: Observations and Interpretation", edited by M. J. Plavec, D. M. Popper, and R. K. Ulrich, p. 109. D. Reidel Publ. Co., Dordrecht.

van Paradijs, J., van der Woerd, H., van der Bij, M., and Lee Van Suu, A., 1982. Astron. Astrophys., 111, 372.

Wilson, R. E., and Devinney, E. J., 1971. Astrophys. J., 166, 605.

Wood, D. B., 1971. Astron. J., 76, 701.

Young, A. T., 1974. In "Methods of Experimental Physics", edited by N. Carleton, vol. 12a, p. 1, p. 95. Academic Press, Inc., New York.

APPENDIX I: LIGHT CURVE NORMAL POINTS

JD - 2 440 000	U MAGNITUDE
5863.5916	11.606 ± 0.041
5864.4502	11.690 ± 0.062
5864.4771	11.562 ± 0.046
5864.5052	11.669 ± 0.022
5864.5356	11.646 ± 0.038
5864.5637	11.614 ± 0.031
5865.2000	11.800 ± 0.040
5865.2200	11.950 ± 0.040
5865.7167	12.554 ± 0.022
5865.7519	12.545 ± 0.025
5865.7775	12.602 ± 0.029
5865.8722	12.802 ± 0.023
5865.9122	12.878 ± 0.042
5865.9384	12.975 ± 0.063
5865.9712	13.107 ± 0.004
5866.1200	13.540 ± 0.040
5866.1500	13.490 ± 0.040
5866.4789	13.937 ± 0.089
5866.5083	13.853 ± 0.053
5866.5348	13.924 ± 0.067

APPENDIX I: (CONTINUED)

JD - 2 440 000	U MAGNITUDE
5866.5685	13.913 ± 0.063
5866.5845	13.911 ± 0.043
5867.4911	13.983 ± 0.050
5867.5190	14.018 ± 0.063
5867.5449	14.088 ± 0.055
5867.5700	14.123 ± 0.054
5868.5201	13.998 ± 0.036
5868.5492	14.026 ± 0.041
5868.5725	14.010 ± 0.049
5874.4829	13.982 ± 0.102
5874.9800	14.220 ± 0.040
5875.0900	13.610 ± 0.040
5875.3992	14.024 ± 0.031
5875.4527	13.896 ± 0.052
5875.5083	13.862 ± 0.054
5875.5234	13.784 ± 0.083
5875.5691	13.911 ± 0.035
5876.2200	13.570 ± 0.040
5876.7170	12.421 ± 0.054
5876.7434	12.370 ± 0.034

APPENDIX I: (CONTINUED)

JD - 2 440 000	U MAGNITUDE
5876.7715	12.330 ± 0.015
5876.8558	12.158 ± 0.010
5876.8948	12.102 ± 0.022
5876.9360	12.025 ± 0.032
5876.9750	11.996 ± 0.006
5877.1000	11.950 ± 0.040
5877.1600	11.900 ± 0.040
5877.1900	11.880 ± 0.040
5877.2200	11.780 ± 0.040
5877.3943	11.773 ± 0.013
5877.4216	11.763 ± 0.013
5877.4453	11.748 ± 0.007
5877.4724	11.746 ± 0.013
5877.4995	11.720 ± 0.007
5877.5138	11.720 ± 0.013
5877.5546	11.704 ± 0.007
5877.5708	11.687 ± 0.008
5878.4078	11.577 ± 0.016
5878.4961	11.594 ± 0.015
5878.5721	11.563 ± 0.010

APPENDIX I: (CONTINUED)

JD - 2 440 000	U MAGNITUDE
5880.4477	11.567 ± 0.016
5880.5053	11.558 ± 0.034

APPENDIX I: (CONTINUED)

JD - 2 440 000	B MAGNITUDE
5863.5916	10.932 ± 0.007
5863.8951	10.947 ± 0.024
5863.9208	10.989 ± 0.039
5864.4500	10.998 ± 0.021
5864.4771	10.918 ± 0.025
5864.5052	10.949 ± 0.031
5864.5356	10.966 ± 0.027
5864.5637	10.956 ± 0.022
5865.2000	11.150 ± 0.020
5865.2200	11.160 ± 0.020
5865.7167	11.538 ± 0.010
5865.7503	11.558 ± 0.022
5865.7520	11.581 ± 0.022
5865.7765	11.663 ± 0.022
5865.7774	11.636 ± 0.036
5865.8165	11.716 ± 0.022
5865.8545	11.736 ± 0.015
5865.8724	11.769 ± 0.002
5865.8938	11.819 ± 0.012
5865.9061	11.821 ± 0.027

APPENDIX I: (CONTINUED)

JD - 2 440 000	B MAGNITUDE
5865.9122	11.842 ± 0.013
5865.9330	11.863 ± 0.014
5865.9382	11.860 ± 0.012
5865.9710	11.906 ± 0.022
5866.1200	12.080 ± 0.020
5866.1500	12.220 ± 0.020
5866.4789	12.366 ± 0.022
5866.5083	12.345 ± 0.010
5866.5348	12.356 ± 0.020
5866.5685	12.348 ± 0.010
5866.5845	12.333 ± 0.023
5866.8240	12.410 ± 0.049
5866.8615	12.381 ± 0.020
5866.8970	12.384 ± 0.048
5866.9153	12.314 ± 0.048
5867.4912	12.425 ± 0.031
5867.5190	12.373 ± 0.014
5867.5447	12.380 ± 0.015
5867.5700	12.405 ± 0.021
5868.5208	12.393 ± 0.008

APPENDIX I: (CONTINUED)

JD - 2 440 000	B MAGNITUDE
5868.5492	12.413 ± 0.017
5868.5725	12.417 ± 0.027
5868.7893	12.460 ± 0.032
5868.8258	12.407 ± 0.032
5869.9416	12.391 ± 0.002
5870.8292	12.395 ± 0.024
5870.8597	12.399 ± 0.022
5872.8225	12.389 ± 0.039
5874.4824	12.442 ± 0.023
5874.9800	12.450 ± 0.020
5875.0900	12.450 ± 0.020
5875.3992	12.387 ± 0.026
5875.4527	12.401 ± 0.010
5875.5083	12.396 ± 0.010
5875.5234	12.402 ± 0.009
5875.5691	12.390 ± 0.008
5875.7621	12.349 ± 0.020
5875.7986	12.368 ± 0.034
5876.2200	12.210 ± 0.020
5876.7174	11.472 ± 0.009

APPENDIX I: (CONTINUED)

JD - 2 440 000	B MAGNITUDE
5876.7233	11.462 ± 0.004
5876.7432	11.440 ± 0.007
5876.7602	11.432 ± 0.011
5876.7715	11.410 ± 0.005
5876.7978	11.400 ± 0.024
5876.8474	11.333 ± 0.038
5876.8556	11.320 ± 0.011
5876.8861	11.290 ± 0.022
5876.8902	11.274 ± 0.022
5876.9194	11.240 ± 0.014
5876.9201	11.246 ± 0.014
5876.9460	11.224 ± 0.003
5876.9468	11.218 ± 0.007
5876.9752	11.211 ± 0.006
5877.1000	11.190 ± 0.020
5877.1600	11.160 ± 0.020
5877.1900	11.120 ± 0.020
5877.2200	11.110 ± 0.020
5877.3942	11.009 ± 0.010
5877.4216	11.008 ± 0.011

APPENDIX I: (CONTINUED)

JD - 2 440 000	B MAGNITUDE
5877.4453	11.001 ± 0.004
5877.4724	10.992 ± 0.008
5877.4995	10.992 ± 0.004
5877.5138	10.989 ± 0.002
5877.5546	10.986 ± 0.006
5877.5708	10.968 ± 0.005
5877.7602	10.940 ± 0.003
5877.8007	10.938 ± 0.022
5877.8386	10.937 ± 0.006
5878.4078	10.915 ± 0.006
5878.4961	10.942 ± 0.004
5878.5721	10.925 ± 0.011
5880.4477	10.915 ± 0.008
5880.5053	10.908 ± 0.006
5908.8607	10.921 ± 0.014
5920.7914	10.926 ± 0.012
5933.7045	10.916 ± 0.014

APPENDIX I: (CONTINUED)

JD - 2 440 000	V MAGNITUDE
5863.5916	9.880 ± 0.003
5863.8778	9.915 ± 0.026
5863.9109	9.915 ± 0.017
5863.9330	9.838 ± 0.019
5864.4500	9.913 ± 0.013
5864.4771	9.860 ± 0.016
5864.5052	9.891 ± 0.017
5864.5356	9.911 ± 0.010
5864.5637	9.888 ± 0.010
5865.2000	9.920 ± 0.010
5865.2200	9.990 ± 0.010
5865.7169	10.086 ± 0.019
5865.7517	10.109 ± 0.016
5865.7774	10.135 ± 0.010
5865.7885	10.122 ± 0.011
5865.8441	10.165 ± 0.011
5865.8710	10.186 ± 0.013
5865.8727	10.182 ± 0.002
5865.8840	10.188 ± 0.008
5865.9123	10.203 ± 0.012

APPENDIX I: (CONTINUED)

JD - 2 440 000	V MAGNITUDE
5865.9124	10.207 ± 0.012
5865.9232	10.220 ± 0.013
5865.9382	10.232 ± 0.018
5865.9712	10.247 ± 0.002
5866.1200	10.330 ± 0.010
5866.1500	10.390 ± 0.010
5866.4798	10.454 ± 0.010
5866.5083	10.434 ± 0.007
5866.5348	10.450 ± 0.008
5866.5685	10.451 ± 0.006
5866.5845	10.468 ± 0.012
5866.8330	10.474 ± 0.017
5866.8708	10.478 ± 0.010
5866.9139	10.482 ± 0.013
5867.4912	10.476 ± 0.006
5867.5190	10.472 ± 0.005
5867.5447	10.483 ± 0.006
5867.5700	10.481 ± 0.005
5868.5201	10.484 ± 0.010
5868.5492	10.485 ± 0.011

APPENDIX I: (CONTINUED)

JD - 2 440 000	V MAGNITUDE
5868.5728	10.484 ± 0.008
5868.7893	10.470 ± 0.014
5868.8258	10.453 ± 0.014
5869.9424	10.500 ± 0.012
5870.7820	10.490 ± 0.011
5870.8051	10.499 ± 0.014
5872.8225	10.492 ± 0.008
5874.4824	10.521 ± 0.012
5874.9800	10.470 ± 0.010
5875.0900	10.510 ± 0.010
5875.3992	10.488 ± 0.018
5875.4519	10.486 ± 0.006
5875.5083	10.490 ± 0.007
5875.5234	10.494 ± 0.007
5875.5691	10.482 ± 0.010
5875.7621	10.474 ± 0.019
5875.7986	10.507 ± 0.006
5876.2200	10.420 ± 0.010
5876.7172	10.082 ± 0.017
5876.7233	10.077 ± 0.010

APPENDIX I: (CONTINUED)

JD - 2 440 000	V MAGNITUDE
5876.7431	10.075 ± 0.015
5876.7602	10.069 ± 0.011
5876.7715	10.059 ± 0.004
5876.7978	10.040 ± 0.008
5876.8448	10.026 ± 0.006
5876.8557	10.018 ± 0.005
5876.8778	10.012 ± 0.011
5876.8896	10.000 ± 0.006
5876.9111	9.988 ± 0.006
5876.9206	9.983 ± 0.008
5876.9444	9.968 ± 0.006
5876.9462	9.970 ± 0.011
5876.9752	9.968 ± 0.010
5877.1000	10.030 ± 0.010
5877.1600	10.030 ± 0.010
5877.1900	10.020 ± 0.010
5877.2200	9.970 ± 0.010
5877.3943	9.917 ± 0.011
5877.4217	9.911 ± 0.005
5877.4453	9.911 ± 0.004

APPENDIX I: (CONTINUED)

JD - 2 440 000	V MAGNITUDE
5877.4724	9.906 ± 0.005
5877.4995	9.908 ± 0.004
5877.5138	9.914 ± 0.011
5877.5546	9.909 ± 0.005
5877.5708	9.894 ± 0.008
5877.7602	9.886 ± 0.007
5877.7986	9.870 ± 0.010
5877.8302	9.864 ± 0.012
5877.8639	9.883 ± 0.013
5878.4078	9.866 ± 0.005
5878.4961	9.883 ± 0.006
5878.5721	9.867 ± 0.003
5880.4477	9.854 ± 0.006
5880.5053	9.847 ± 0.007
5908.8607	9.861 ± 0.013
5920.7914	9.857 ± 0.008
5933.7045	9.832 ± 0.010

APPENDIX II: (O-C)'s FOR LIGHT CURVE SOLUTIONS

Θ (°)	OBSERVED U	CALCULATED U	O-C
6.899	13.570	13.631	-0.061
6.942	13.490	13.613	-0.123
6.983	13.540	13.496	+0.044
7.188	13.107	13.108	-0.001
7.233	12.975	12.998	-0.023
7.269	12.878	12.943	-0.065
7.324	12.802	12.816	-0.014
7.454	12.602	12.635	-0.033
7.489	12.544	12.599	-0.055
7.537	12.554	12.503	+0.051
7.581	12.421	12.446	-0.025
7.618	12.370	12.418	-0.048
7.657	12.330	12.359	-0.029
7.773	12.158	12.228	-0.070
7.826	12.102	12.192	-0.090
7.883	12.025	12.131	-0.106
7.936	11.996	12.096	-0.100
8.108	11.950	11.950	0.000
8.191	11.900	11.909	-0.009
8.220	11.950	11.881	+0.069

APPENDIX II: (CONTINUED)

θ (°)	OBSERVED U	CALCULATED U	O-C
8.232	11.880	11.887	-0.007
8.247	11.800	11.874	-0.074
8.273	11.780	11.865	-0.085
8.512	11.773	11.771	+0.002
8.550	11.763	11.761	+0.002
8.583	11.748	11.748	0.000
8.620	11.746	11.740	+0.006
8.657	11.720	11.738	-0.018
8.677	11.720	11.735	-0.015

APPENDIX II: (CONTINUED)

θ (°)	OBSERVED B	CALCULATED B	O-C
6.899	12.210	12.298	-0.088
6.942	12.220	12.241	-0.021
6.983	12.080	12.190	-0.110
7.188	11.906	11.937	-0.031
7.233	11.860	11.893	-0.033
7.240	11.863	11.885	-0.022
7.269	11.842	11.858	-0.016
7.277	11.821	11.834	-0.013
7.294	11.819	11.821	-0.002
7.323	11.769	11.790	-0.021
7.348	11.736	11.756	-0.020
7.400	11.716	11.694	+0.022
7.454	11.636	11.637	-0.001
7.455	11.663	11.611	+0.052
7.489	11.581	11.594	-0.013
7.491	11.558	11.592	-0.034
7.537	11.538	11.536	+0.002
7.582	11.472	11.488	-0.016
7.590	11.462	11.480	-0.018
7.618	11.440	11.465	-0.025

APPENDIX II: (CONTINUED)

θ (°)	OBSERVED B	CALCULATED B	O-C
7.641	11.432	11.439	-0.007
7.657	11.410	11.430	-0.020
7.693	11.400	11.393	+0.007
7.761	11.333	11.327	+0.006
7.772	11.320	11.319	+0.001
7.814	11.290	11.297	-0.007
7.820	11.274	11.280	-0.006
7.860	11.240	11.250	-0.010
7.861	11.246	11.249	-0.003
7.896	11.224	11.235	-0.011
7.900	11.218	11.218	0.000
7.936	11.211	11.203	+0.008
8.108	11.190	11.099	+0.091
8.191	11.160	11.066	+0.094
8.220	11.160	11.060	+0.100
8.232	11.120	11.053	+0.067
8.247	11.150	11.048	+0.102
8.273	11.110	11.045	+0.065

APPENDIX II: (CONTINUED)

Θ (°)	OBSERVED V	CALCULATED V	O-C
6.488	10.454	10.483	-0.029
6.899	10.420	10.378	+0.042
6.942	10.390	10.354	+0.036
6.983	10.330	10.344	-0.014
7.188	10.247	10.251	-0.004
7.233	10.232	10.234	-0.002
7.253	10.220	10.218	+0.002
7.268	10.208	10.213	-0.005
7.269	10.203	10.213	-0.010
7.308	10.188	10.194	-0.006
7.323	10.182	10.190	-0.008
7.325	10.186	10.189	-0.003
7.362	10.165	10.170	-0.005
7.439	10.122	10.145	-0.023
7.454	10.135	10.140	-0.005
7.489	10.109	10.121	-0.012
7.537	10.086	10.107	-0.021
7.582	10.082	10.084	-0.002
7.590	10.077	10.081	-0.004
7.618	10.075	10.073	+0.002

APPENDIX II: (CONTINUED)

θ (°)	OBSERVED V	CALCULATED V	O-C
7.641	10.069	10.060	+0.009
7.657	10.059	10.055	-0.004
7.693	10.040	10.047	-0.007
7.757	10.026	10.028	-0.002
7.773	10.018	10.023	-0.005
7.803	10.012	10.012	0.000
7.819	10.000	10.007	-0.007
7.849	9.988	9.996	-0.008
7.861	9.983	9.990	-0.007
7.894	9.968	9.981	-0.013
7.897	9.970	9.979	-0.009
7.936	9.967	9.972	-0.005
8.108	10.030	9.934	+0.096
8.191	10.030	9.920	+0.110
8.220	9.990	9.916	+0.074
8.232	10.020	9.915	+0.105
8.247	9.920	9.912	+0.008
8.273	9.970	9.909	+0.061

VITA

Surname: KNEE Given Names: LEWIS BENJAMIN GRAHAM

Place of Birth: Corner Brook, N.F.L.D. Date of Birth: Nov. 12, 1961

Educational Institutions Attended, with Dates of Entering and Leaving:

MEMORIAL UNIVERSITY OF NEWFOUNDLAND, ST. JOHN'S, N.F.L.D. 1978 to 1983

UNIVERSITY OF VICTORIA, VICTORIA, B.C. 1983 to 1985

Degrees, Diplomas, Etc., Awarded, with Dates and Names of Institutions:

B.Sc. (Honours) 1983 MEMORIAL UNIVERSITY OF NEWFOUNDLAND, ST. JOHN'S

Honours and Awards:

Dr. A. Barnes Scholarship, 1980-81

N.S.E.R.C. Summer Undergraduate Research Award, 1981

Centenary of Responsible Government Scholarship, 1981-82

N.S.E.R.C. Summer Undergraduate Research Award, 1982

Dr. W. W. Blackall Scholarship, 1982-83

Memorial University of Newfoundland Medal in Physics, 1983

N.S.E.R.C. Summer Undergraduate Research Award, 1983

N.S.E.R.C. Postgraduate Scholarship, 1983-85

R. M. Petrie Memorial Fellowship, 1984-85

N.S.E.R.C. Postgraduate Scholarship, 1985-87

Government of Finland Scholarship, 1985-86

Publications:

Whitmore, M. D., Hare, I. P., and Knee, L. B. G., 1982. Phys. Rev., 27, 3733.

Knee, L. B. G., 1983. B.Sc. Thesis, Memorial University of Newfoundland.

Robb, R. M., and Knee, L. B. G., 1984. I. A. U. Circ., No. 3976.

PARTIAL COPYRIGHT LICENSE

I hereby grant the right to lend my thesis or dissertation (the title of which is shown below) to users of the University of Victoria Library, and to make single copies only for such users or in response to a request from the Library of any other university, or similar institution, on its behalf or for one of its users. I further agree that permission for extensive copying of this thesis for scholarly purposes may be granted by me or a member of the University designated by me. It is understood that copying or publication of this thesis for financial gain shall not be allowed without my written permission.

Title of Thesis/Dissertation

A NEW MODEL OF THE ECLIPSING SYSTEM RZ OPHIUCHI

Author [redacted]

LEWIS B. G. KNEE